LA-UR-22-24977
Approved for public release; distribution is unlimited.

Title: Spring 2022 update on the status of the Local Wavenumber Model (LWN) in xRAGE

Author(s): Braun, Noah Oakley
Canfield, Jesse M.
Saenz, Juan Antonio

Intended for: Report

Issued: 2022-05-31

Los Alamos NATIONAL LABORATORY

Spring 2022 update on the status of the Local Wavenumber Model (LWN) in xRAGE

N. O. Braun; J. A. Saenz; J. Canfield

XCP / XTD, Los Alamos National Laboratory, Los Alamos, NM, USA

Abstract

An updated implementation of the Local Wavenumber Model (LWN) is discussed, primarily differing from recent versions [1] by placing a greater focus on capturing a wide variety of turbulent flows including compressible flows. New models are introduced for spectral backscatter effects, the effect of bulk compression on the spectra, and incorporating the multispecies variables tracked in BHR4 [2]. Methods for reducing the compurational expense of tracking spectra for turbulent quantites are also investigated. Like recent versions of BHR [3, 4, 2], we test LWN in a number of canonical flows using a single set of coefficients, but additional coefficient tuning is likely to be required to improve the agreement with some of these flows.

Contents

1. Background

Turbulent flows play an important role in the mixing of materials in many problems of interest, and modeling the development and evolution of turbulent presents a significant difficulty. The Besnard-Harlow-Rauenzahn (BHR) models [5, 6, 3, 4, 2] have shown significant progress in modeling variable density turbulence in compressible flows, but retain certain shortcoming, particularly in the handling of initial conditions that develop from a laminar state. Tracer-based modal modeling [7, 8, 9] has aided in modeling transitional flows, but neither the BHR turbulence models nor the available laminar modal models are well suited for the transitional stages of a flow.

Spectral models, particularly the proposed Local Wavenumber (LWN) model [1, 10, 11, 12], have seen renewed interest due to their ability to better address transitional flows in a physical manner. The models are developed off of many historical models [13, 14, 15, 16], but further work is needed to produce models that work across a broad range of compressible, multi-material flows without case-by-base tuning. Simple preliminary models for phenomena such as compression and backscatter are presented to aid in this regard.

The purpose of this report is to document updates to the version of LWN currently implemented in the xRage hydrocode, as an extension of the documentation in the previous L3 milestone [11]. The development of the modeled equations is discussed in section 2. Physics changes to the model relative to previous xRage version of LWN [11] are presented in sections 2.1 through 2.3. The implementation of LWN in xRage is currently closely tied to the BHR3.1 implementation, and equations for the LWN variables rationalizing this similarity are developed in sections 2.4 through 2.6. A relatively cost-effective approach to numerical spectral updates is presented in section 3. Although coefficients tuning and closure development are not finalized, the preliminary model presented here is tested in a number of canonical flows in section 4 to illustrate that it can behave in a relatively robust manner in inhomogeneous and compressible flows.

2. Model Construction

The approach here is to represent the two-point LWN model following the definitions and approach from BHR3.1's [3] single point equations as much as possible. This is useful because it separates one-point production/destruction terms from spectral terms, which potentially makes the role of the new two-point terms easier to interpret. Additionally, the one-point BHR3.1 form is well tested and relatively stable, and this form allows some models developed for BHR3.1 to be applied to LWN.

We start by defining the following variables,

$$R_{ij}(\boldsymbol{x},\boldsymbol{r}) = \frac{\overline{\rho\left(\boldsymbol{x}+\frac{\boldsymbol{r}}{2}\right) u_i''\left(\boldsymbol{x}-\frac{\boldsymbol{r}}{2}\right)\ u_n''\left(\boldsymbol{x}+\frac{\boldsymbol{r}}{2}\right)}}{\bar{\rho}\left(\boldsymbol{x}+\frac{\boldsymbol{r}}{2}\right)} \tag{1}$$

$$b(\boldsymbol{x},\boldsymbol{r}) = -\overline{\rho'\left(\boldsymbol{x}+\frac{\boldsymbol{r}}{\boldsymbol{2}}\right) v'\left(\boldsymbol{x}-\frac{\boldsymbol{r}}{2}\right)} \tag{2}$$

$$a_n(\boldsymbol{x},\boldsymbol{r}) = \frac{\overline{\rho'\left(\boldsymbol{x}+\frac{\boldsymbol{r}}{2}\right) u_n''\left(\boldsymbol{x}-\frac{\boldsymbol{r}}{2}\right)}}{\bar{\rho}\left(\boldsymbol{x}-\frac{\boldsymbol{r}}{2}\right)} \tag{3}$$

There are numerous different ways to define these correlations, for instance forms similar to $R_{ij}(\boldsymbol{x},\boldsymbol{r}) = \overline{\rho(\boldsymbol{x})u_i''(\boldsymbol{x})\ u_n''(\boldsymbol{x}+\boldsymbol{r})}/\bar{\rho}(\boldsymbol{x})$ are quite common. Most forms don't make a significant difference once final assumptions have been made, and although some forms enforce useful symmetry properties such as $R_{ij}(\boldsymbol{x},\boldsymbol{r}) = R_{ji}(\boldsymbol{x},\boldsymbol{r})$ these generally come at the cost of increased complexity. Single point values used in models such as BHR [3] are denoted $R_{ij}(\boldsymbol{x})$, noting that $R_{ij}(\boldsymbol{x}) = R_{ij}(\boldsymbol{x},\boldsymbol{r}=0)$. Clark and Zemach [16] use a similar form based on $\boldsymbol{x}\pm\frac{\boldsymbol{r}}{2}$, and it can be view as appropriate for turbulence modeling in some regards because it represents correlations in the vicinity of x, rather than the correlation of x with nearby points.

We generally seek Fourier-space solutions, and to reduce the dimensionality solve for shell-summed quantities e.g. $R_{ij}(\boldsymbol{x},k_r) = \int_{\phi=0}^{2\pi}\int_{\theta=0}^{\pi}\mathcal{F}\left(R_{ij}(\boldsymbol{x},\boldsymbol{r})\right)k_r^2\sin(\theta)\,d\theta d\phi$, where the Fourier transform is $g(\boldsymbol{k}) = \mathcal{F}(g(\boldsymbol{r}))$. The single point correlations are integrals over the shell integrals, e.g. $R_{ij}(\boldsymbol{x}) = \int_0^\infty R_{ij}(\boldsymbol{x}, k_r)dk_r$. The final results are only dependent on the radial wavenumber and so as a shorthand we drop the subscript, $R_{ij}(\boldsymbol{x}, k) = R_{ij}(\boldsymbol{x}, k_r)$.

2.1. Modeling Cascade terms with backscatter

LWN [10, 1] has typically modeled the cascade of energy towards fine scales using an advection-diffusion model similar to that of Leith,

$$\frac{\partial \bar{\rho}(\boldsymbol{x}) R_{ij}(\boldsymbol{x}, \boldsymbol{r})}{\partial t} = \bar{\rho}(\boldsymbol{x}) \frac{\partial}{\partial k}\left[k\, \theta^{-1}(\boldsymbol{x}, k)\left[-C'_{r1} R_{ij}(\boldsymbol{x}, k) + C'_{r2} k \frac{\partial R_{ij}(\boldsymbol{x}, k)}{\partial k}\right]\right] \tag{4}$$

Where θ^{-1} is a turbulent frequency defined by

$$\theta^{-1}(\boldsymbol{x}) = \left(\int_0^k k^2 R_{nn}(\boldsymbol{x}, k) dk\right)^{\frac{1}{2}} \tag{5}$$

The form of this frequency ensures that the flux of energy over k is constant in a $R_{nn}(\boldsymbol{x}, k) \propto k^{-\frac{5}{3}}$ spectrum, consistent with the slope seen in the spectra of high Reynolds number isotropic turbulence. Here, we use the same fundamental form, but introduce an additional frequency associated with backscatter processes $\theta_{back}^{-1}(\boldsymbol{x}, k)$,

$$\frac{\partial \bar{\rho}(\boldsymbol{x}) R_{ij}(\boldsymbol{x}, \boldsymbol{r})}{\partial t} = \bar{\rho}(\boldsymbol{x}) \frac{\partial}{\partial k}\left[k\left(\theta^{-1}(\boldsymbol{x}, k) + \theta_{back}^{-1}(\boldsymbol{x}, k)\right)\left[-C'_{r1} R_{ij}(\boldsymbol{x}, k) + C'_{r2} k \frac{\partial R_{ij}(\boldsymbol{x}, k)}{\partial k}\right]\right] \tag{6}$$

The backscatter frequency is assumed to be of the same form as $\theta^{-1}(\boldsymbol{x}, k)$, but integrated over large wavenumbers, namely,

$$\theta_{back}^{-1}(\boldsymbol{x}, k) \propto \left(\int_k^\infty \sqrt{(k')^{-m} R_{nn}(\boldsymbol{x}, k')} dk'\right) \tag{7}$$

The scaling in $\theta_{back}^{-1}(\boldsymbol{x}, k)$ is assumed to yield a uniform advection velocity in a k^4 spectrum, which requires $k\theta_{back}^{-1}(\boldsymbol{x}, k) R_{ij}(\boldsymbol{x}, k)$ and $k^2\theta_{back}^{-1}(\boldsymbol{x}, k)\, \partial R_{ij}(\boldsymbol{x}, k)/\partial k$ to be constant if $R_{ij}(\boldsymbol{x}, k) \propto k^4$. Assuming $\theta_{back}^{-1}(\boldsymbol{x}, k)$ scales with the integral lengthscale for incompressible isotropic turbulence, L_I, this yields,

$$\theta_{back}^{-1}(\boldsymbol{x}, k) = (L_I)^{-\frac{17}{2}} \int_k^\infty \sqrt{(k')^{-15} R_{nn}(\boldsymbol{x}, k')} dk' \tag{8}$$

$$L_I = \frac{3\pi}{4} \frac{\int_0^\infty k^{-1} R_{nn}(\boldsymbol{x}, k) dk}{\int_0^\infty R_{nn}(\boldsymbol{x}, k) dk} \tag{9}$$

Additionally, there should not be a constant flux of energy towards large wavenumbers, as this would produce a pile up of energy at the lower wavenumber bound. The flux from the backscatter term should vanish for $R_{ij}(\boldsymbol{x}, k) \propto k^4$,

$$-C'_{r1} k \theta_{back}^{-1}(\boldsymbol{x}, k) R_{ij}(\boldsymbol{x}, k) + C'_{r2} \theta_{back}^{-1}(\boldsymbol{x}, k) k^2 \frac{\partial R_{ij}(\boldsymbol{x}, k)}{\partial k} = 0 \; if \; R_{ij}(\boldsymbol{x}, k) \propto k^4 \tag{10}$$

This requires that $C'_{r1} = 4C'_{r2}$, and this relation also holds for the cascade of the other variables $a_i(\boldsymbol{x}, k)$ and $b(\boldsymbol{x}, k)$. However, the very large power of k^{-15} means the turbulent backscatter frequency can become pathological in the low-k tail on the spectrum. To stabilize this, we currently limit the backscatter frequency based on the condition number on the update of k-space energy,

$$\theta_{back}^{-1}(\boldsymbol{x}, k) \frac{\Delta t}{\Delta z^2} \leq 10^6 \tag{11}$$

The backscatter form is ad hoc, but reliably produces a k^4 regime in the low wavenumbers of the R_{nn} spectrum when initialized from top-hat initial condition spectra. EDQNM offers alternative models for backscatter [17] that are likely more physical, but the simple advection-diffusion form of the Leith model is useful, particularly when considering issues such as numerical stability. Clark and Spitz [15] also propose a backscatter model for a_i abd b that is effectively the forward cascade model but with a reversed advection direction. These models remove the adhoc dependence on integral lengthscale, but it was found to be difficult to enforce that the transport of energy goes to zero at the lower k-

space boundary in preliminary testing. These problems could likely be overcome and using an advection model for backscatter should not be ruled out.

Example spectra from an $A_t = 0.5$ Rayleigh-Taylor simulation are shown in Figure 1 with and without the backscatter term. When the initial condition does not contain significant amounts of energy at the low wavenumbers, the case without backscatter tends to retain the steep slope at low wavenumbers, whereas the backscatter model forces it to relax to a k^4 spectrum. Although the k^4 spectrum at low wavenumbers is not universal, having some energy content at the large scales is typically realistic. The large scales are also a disproportionately large fraction of the turbulent viscosity, and the backscatter term can significantly affect the statistics of the mixing layer, as shown in Figure 2. The additional of the backscatter term has no noticeable effect at early times but has a significant impact on the late time growth of the mixing layer.

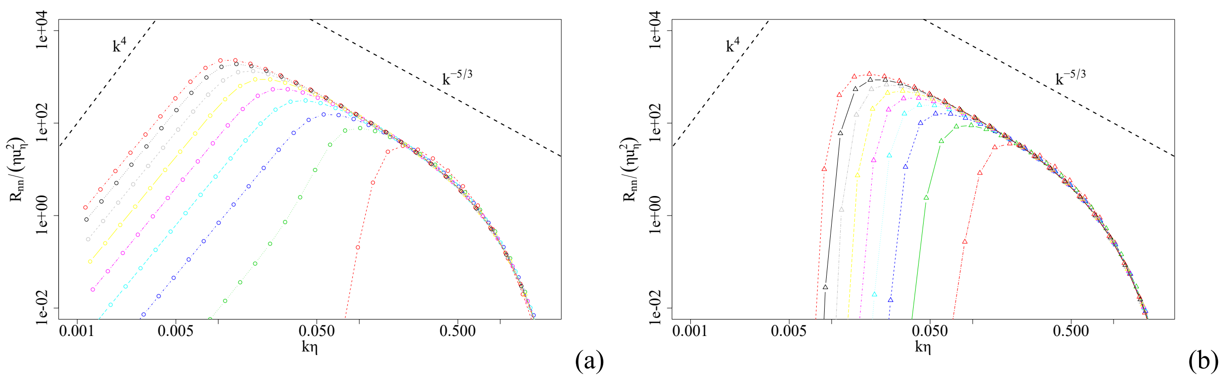

Figure 1 – Spectra of R_{nn} in an $A_t = 0.5$ Rayleigh-Taylor simulation with the backscatter term θ_{back}^{-1} (a), or without the backscatter term (b). The spectra are sampled at the center of the mixing layer layer. Each line corresponds to a different time, with later times being lines further left on the plots.

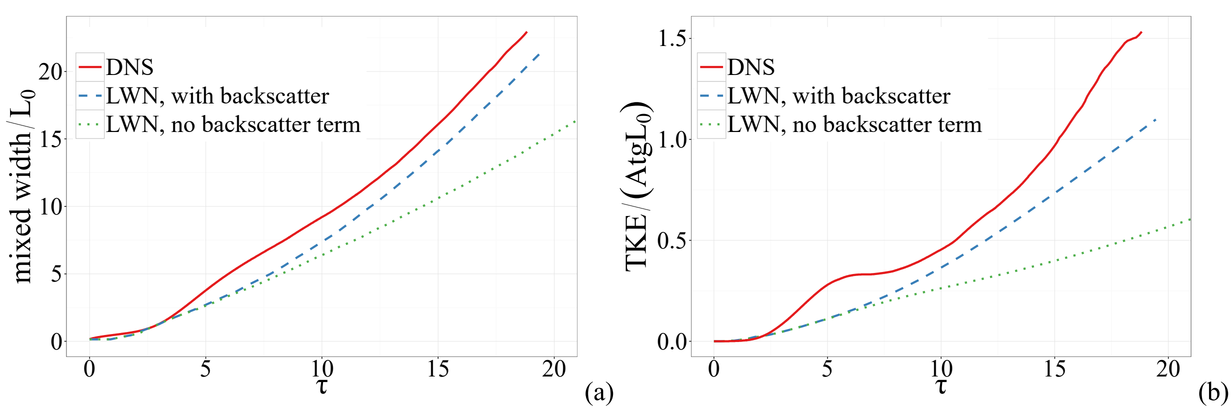

Figure 2 – Mixed width(a) and turbulent kinetic energy (b) in an $A_t = 0.5$ Rayleigh-Taylor simulation with and without the backscatter term θ_{back}^{-1}. The DNS is from Livescu et al. [18]. Note that this image to highlight effect of the backscatter term, and coefficient tuning could bring the without backscatter case closer to the DNS.

2.2. Modeling the effect of bulk compression on spectra

Recent two-point turbulence models, e.g. [1], have mostly considered incompressible flows and have not needed to consider the effects of phenomena such as shocks on the turbulent scales. Compressing turbulence will tend to reduce the scales that describe the turbulence, and capturing this effect is important for high compression ratio flows. For simplicity, we currently model the effects of bulk compression as an isotropic spectral-advection model

$$\frac{\partial \bar{\rho}(\boldsymbol{x})R_{ij}(\boldsymbol{x},\boldsymbol{r})}{\partial t} = C_{comp}\bar{u}_{n,n}\frac{\partial}{\partial k}\left[kR_{ij}(\boldsymbol{x},k)\right] \tag{12}$$

The coefficient $C_{comp} = 1/3$ is taken be the same as the scaling of the Taylor lengthscale with velocity dilatation in rapid distortion theory (RDT) of spherical compressions [19]. One does not expect compression to behave in an isotropic manner, for instance RDT predicts an axial compression in the 1-direction will compress the wavenumbers of the transverse solenoidal fluctuations associated with R_{22} and R_{33}, but not R_{11} [20]. Capturing this anisotropic effect on compression is likely important in reproducing some of the more complex behaviors seen in DNS, such as the trend to towards a temporally increasing anisotropy in the single-point Reynolds stress tensor after shocks in RM simulations [21]. Unfortunately constructing a model that reproduces this anisotropy is difficult, particularly in spherical or cylindrical coordinate systems. Clark [16] proposed a more complex model for general flow cases included shear, which may be useful if stretching and compressing of the spectra is found to be important in general problems.

2.3. Modeling single-point multispecies variables

The multispecies variables tracked in BHR4 [2] track the fluctuations in mass fraction of each material, b^k, or the turbulent flux of mass fraction of each material, a^k. These variables are defined,

$$a_i^k(x) = -\frac{\overline{\rho(x)c^{k''}(x)u_i''(x)}}{\bar{\rho}(x)} \tag{13}$$

$$b^k(x) = \overline{c^{k''}(x)} \tag{14}$$

These multispecies terms previously have helped the BHR model capture certain types of stabilized interfaces [2], and likely provide a more accurate approach to material transport than the gradient diffusion models used in many turbulence models. While two-point models for a^k and b^k could be developed, it would likely be pathologically expensive to evolve them because separate spectra for a^k and b^k would need to be tracked for each material. However, in incompressible flows these multispecies terms can be related to the density terms tracked in LWN,

$$a_i = \bar{\rho}\sum_k \frac{a_i^k}{\rho^k}, \qquad b = \bar{\rho}\sum_k \frac{b^k}{\rho^k}, \qquad \frac{1}{\bar{\rho}} = \sum_k \frac{\tilde{c}^k}{\rho^k}, \tag{15}$$

Which suggests that if ρ^k is roughly uniform then the multispecies terms a_i^k and b^k should have similar spectra distributions to the density weighted terms tracked in LWN, a_i and b. Tracking spectral equations for each material with a_i^k and b^k would be cost prohibitive, so the single point equations for a_i^k and b^k from BHR4 are retained [2]. These single point equations are still solvable because single point terms can easily be calculated from the two-point terms in LWN, for example $R_{ij}(\boldsymbol{x})$ is the integral of $R_{ij}(\boldsymbol{x},k)$. The one term that can't be used from BHR4 is the dissipation rate of a_i^k and b^k, because these terms were closed using the dissipation lengthscale that was tracked in BHR but is no longer tracked in LWN. Noting the relations (15), we assumed the dissipation for a^k scales linearly with the dissipation of a_i,

$$\varepsilon_{a^k} \approx a_j^k(x)\frac{\varepsilon_a}{a_j(x)} \tag{16}$$

$$\varepsilon_{b^k} \approx b^k(x)\frac{\varepsilon_b}{b(x)} \tag{17}$$

Where a_i and the dissipation rate of a_i, ε_a, (including interactions with the spectral boundary conditions) are computed from the LWN equations. An alternative approach would be to assume spectra of the form (**which is not used here**),

$$a_j^k(x,k) \approx a_j^k(x)\frac{|a_j(x,k)|}{\int_0^\infty |a_j(x,k')|\,dk'} \tag{18}$$

$$b^k(x,k) \approx b^k(x)\frac{|b(x,k)|}{\int_0^\infty |b(x,k')|\,dk'} \tag{19}$$

And then calculate ε_{a^k} based on the cascade of $a_j^k(x,k)$. The absolute values of the spectra are needed for stability, but this may incur some error if, for example, the sign of $a_j(x,k)$ is positive at large scales and negative at small scales. This spectral approach isn't currently used due to being more computationally expensive. We use the same single point equations for a_i^k and b^k from BHR4 [2], but with decay terms that match the two-point a and b tracked in LWN, relative to the summation relations of (15)

$$\begin{aligned}\frac{\partial\bar{\rho}(\boldsymbol{x})a_i^k(\boldsymbol{x})}{\partial t} &+ \left(\bar{\rho}(\boldsymbol{x})\tilde{u}_j(\boldsymbol{x})a_i^k(\boldsymbol{x})\right)_{,j}\\ &= (1-C_{ap})b^k(\boldsymbol{x})\bar{P}_{,i}(\boldsymbol{x}) + \bar{\rho}(\boldsymbol{x})\tilde{R}_{ij}(\boldsymbol{x})\tilde{c}^k_{,j} - (1-C_{au})\bar{\rho}(\boldsymbol{x})a_j^k(\boldsymbol{x})\bar{u}_{i,j}(\boldsymbol{x})\\ &+ a_i(\boldsymbol{x})\left(\bar{\rho}(\boldsymbol{x})a_j^k(\boldsymbol{x})\right)_{,j} + C_d\bar{\rho}(\boldsymbol{x})\left(\nu_t(\boldsymbol{x})a_i^k(\boldsymbol{x})\right)_{,n} - a_j^k(x)\frac{\varepsilon_a}{a_j(\boldsymbol{x})}\end{aligned} \tag{20}$$

$$\begin{aligned}\frac{\partial\bar{\rho}(\boldsymbol{x})b^k(\boldsymbol{x})}{\partial t} &+ \left(\bar{\rho}(\boldsymbol{x})\tilde{u}_j(\boldsymbol{x})b^k(\boldsymbol{x})\right)_{,j}\\ &= \bar{\rho}a_j(\boldsymbol{x})\left(\tilde{c}^k(\boldsymbol{x}) + 2b^k(\boldsymbol{x})\right)_{,j} + \bar{\rho}(\boldsymbol{x})b^k(\boldsymbol{x})a_{j,j}(\boldsymbol{x}) - a_j^k(\boldsymbol{x})\bar{\rho}_{,j}(\boldsymbol{x})\\ &+ C_d\bar{\rho}(\boldsymbol{x})\left(\nu_t(\boldsymbol{x})b^k(\boldsymbol{x})\right)_{,n} - b^k(\boldsymbol{x})\frac{\varepsilon_b}{b(\boldsymbol{x})}.\end{aligned} \tag{21}$$

2.4. $\boldsymbol{R_{ij}}$ Equation

Given that we are developing the xRage version of LWN based on the construction of BHR, it is useful to develop corresponding unclosed equations that follow BHR's form. Many other forms for two-point turbulent statistics have been derived [22, 15, 12, 14], but the form used here is specifically derived to trivially reduce the unclosed BHR equations in the single point limit $r \to 0$. This is a fairly simple process because if one follows the same steps used to derive unclosed BHR equations e.g. [4], but retains two separate spatial evaluation points in the initial equations, this will yield a set of equations that asymptote to the BHR equations in the limit of the two evaluation points becoming equal. The unclosed BHR equations are relatively well understood, and it naturally separates quantities that produce turbulent kinetic energy (terms that are non-zero as $r \to 0$) from terms that only effect the spectral shape of the Reynolds stress (terms that are zero for $r \to 0$).

To obtain a transport equation for $R_{ij}(x,r)$, we multiple the transport equations for u'' and $\rho u''$, evaluated at $x - \frac{r}{2}$ and $x + \frac{r}{2}$ respectively, [15]

$$\frac{\partial u_i''}{\partial t} + u_n''(\tilde{u}_i + u_i'')_{,n} + \tilde{u}_n u_{i,n}'' = \left(\bar{v} - \frac{1}{\bar{\rho}}\right)\bar{\sigma}_{ni,n} + v'\bar{\sigma}_{ni,n} + v\sigma'_{ni,n} + \frac{1}{\bar{\rho}}(\bar{\rho}R_{ni})_{,n} \tag{22}$$

$$\frac{\partial\rho u_i''}{\partial t} + \left(\rho u_i''(\tilde{u}_n + u_n'')\right)_{,n} + \rho u_n''\tilde{u}_{i,n} = \sigma'_{ni,n} - \frac{\rho'}{\bar{\rho}}\bar{\sigma}_{ni,n} + \left(1 + \frac{\rho'}{\bar{\rho}}\right)(\bar{\rho}R_{ni})_{,n} \tag{23}$$

For the full derivation see Appendix A.1. To simplify the results, we make the following assumptions:

- Neglect mean flow viscous stresses so $\bar{\sigma}_{ij} \approx -\bar{P}\delta_{ij}$
- The assumption is made that mean flow quantities can be approximated by their local values, for example $\bar{\rho}(x \pm r/2) \approx \bar{\rho}(x)$. This is accurate for homogenous flows, but neglects certain physics of inhomogeneous flows. Other studies have used Taylor expansions such as $\bar{\rho}(x \pm r/2) \approx \bar{\rho}(x) \pm \frac{r}{2}\frac{d\bar{\rho}(x)}{dx}$, but in compressible flows with shocks present this could easily approximate negative densities or other nonphysical behavior. In these cases, there does not appear to be any obvious to way to directly approximate nonlocal values without using a nonlocal, and computationally impractical, method or modeling these effects in a term-by-term manner. Clark and Zemach [16] provides a model for these 'mean flow coupling' terms in the R_{ij} equation in an incompressible case, but that also becomes quite complex. The one case where we do not neglect these

terms is in compression of the spectra. Shock-driven compression moves energy in the spectra towards smaller scales, and is a result of inhomogeneity in the mean velocity field (specifically it seems the term $\{\overline{\rho(x+r/2)u_j''(x+r/2)u_{i,n}''(x-r/2)}\big(\tilde{u}_n(x+r/2)-\tilde{u}_n(x-r/2)\big)\}$).

Under these assumptions, we obtain a form of the $R_{ij}(x,r)$ that reduces to the $R_{ij}(x)$ form used by BHR3.1 [3, 4] if evaluated at $r=0$. For simplicity, and to maintain that all terms individually $\to 0$ as $r\to\infty$, we write the equations with a slightly different form of the transport term. The naming of terms follows the naming from BHR [4], though because of the 2-point nature of these equations the terms make take on additional physics.

$$\begin{aligned}\frac{\partial\bar{\rho}(\boldsymbol{x})R_{ij}(\boldsymbol{x},\boldsymbol{r})}{\partial t}&+\left(\bar{\rho}(\boldsymbol{x})R_{ij}(\boldsymbol{x},\boldsymbol{r})\tilde{u}_n(\boldsymbol{x})\right)_{,n}\\&=\Gamma_{prod}(\boldsymbol{x},\boldsymbol{r})+\Gamma_{trans}(\boldsymbol{x},\boldsymbol{r})+\Gamma_{pstrain+diss}(\boldsymbol{x},\boldsymbol{r})+\sum_{i=1}^{4}\Gamma_i(\boldsymbol{x},\boldsymbol{r})\end{aligned}\tag{24}$$

The production term is,

$$\Gamma_{prod}(\boldsymbol{x},\boldsymbol{r})=-\bar{\rho}(\boldsymbol{x})R_{in}(\boldsymbol{x},\boldsymbol{r})\tilde{u}_{j,n}(\boldsymbol{x})-\bar{\rho}(\boldsymbol{x})R_{nj}(\boldsymbol{x},\boldsymbol{r})\tilde{u}_{i,n}(\boldsymbol{x})+\ a_i(\boldsymbol{x},\boldsymbol{r})\bar{P}_{,j}(\boldsymbol{x})+a_j(\boldsymbol{x},-\boldsymbol{r})\bar{P}_{,i}(\boldsymbol{x})\tag{25}$$

The transport term is,

$$\begin{aligned}\Gamma_{trans}(\boldsymbol{x},\boldsymbol{r})=&-\left(\overline{\rho\left(\boldsymbol{x}+\frac{\boldsymbol{r}}{2}\right)u_i'\left(\boldsymbol{x}-\frac{\boldsymbol{r}}{2}\right)u_j''\left(\boldsymbol{x}+\frac{\boldsymbol{r}}{2}\right)u_n''\left(\boldsymbol{x}+\frac{\boldsymbol{r}}{2}\right)}\right)_{,n}\\&+\left(\overline{u_i''\left(\boldsymbol{x}-\frac{\boldsymbol{r}}{2}\right)\sigma_{nj}'\left(\boldsymbol{x}+\frac{\boldsymbol{r}}{2}\right)}+\overline{\rho\left(\boldsymbol{x}+\frac{\boldsymbol{r}}{2}\right)\nu\left(\boldsymbol{x}-\frac{\boldsymbol{r}}{2}\right)u_j''\left(\boldsymbol{x}+\frac{\boldsymbol{r}}{2}\right)\sigma_{ni}'\left(\boldsymbol{x}-\frac{\boldsymbol{r}}{2}\right)}\right)_{,n}\\&+a_i(\boldsymbol{x},\boldsymbol{r})\left(\bar{\rho}(\boldsymbol{x})R_{nj}(\boldsymbol{x},0)\right)_{,n}+\bar{\rho}(\boldsymbol{x})R_{nj}(\boldsymbol{x},\boldsymbol{r})a_{i,n}(\boldsymbol{x},0)\end{aligned}\tag{26}$$

The pressure strain and dissipation terms are,

$$\Gamma_{pstrain+diss}(\boldsymbol{x},\boldsymbol{r})=-\overline{\left(\rho\left(\boldsymbol{x}+\frac{\boldsymbol{r}}{2}\right)\nu\left(\boldsymbol{x}-\frac{\boldsymbol{r}}{2}\right)u_j''\left(\boldsymbol{x}+\frac{\boldsymbol{r}}{2}\right)\right)_{,n}\sigma_{ni}'\left(\boldsymbol{x}-\frac{\boldsymbol{r}}{2}\right)}-\overline{u_{i,n}''\left(\boldsymbol{x}-\frac{\boldsymbol{r}}{2}\right)\sigma_{nj}'\left(\boldsymbol{x}+\frac{\boldsymbol{r}}{2}\right)}\tag{27}$$

The remaining terms have no net effect on the mean values and do not show up in the single point equations, $\Gamma_i(\boldsymbol{x},0)=0$. Note that these often are in the form of a structure function-like term multiplied with a gradient.

$$\Gamma_1(\boldsymbol{x},\boldsymbol{r})=\overline{\rho\left(\boldsymbol{x}+\frac{\boldsymbol{r}}{\mathbf{2}}\right)u_j''\left(\boldsymbol{x}+\frac{\boldsymbol{r}}{\mathbf{2}}\right)u_{i,n}'\left(\boldsymbol{x}-\frac{\boldsymbol{r}}{\mathbf{2}}\right)\left[u_n''\left(\boldsymbol{x}+\frac{\boldsymbol{r}}{\mathbf{2}}\right)-u_n''\left(\boldsymbol{x}-\frac{\boldsymbol{r}}{\mathbf{2}}\right)\right]}\tag{28}$$

$$\Gamma_2(\boldsymbol{x},\boldsymbol{r})=-\left(\overline{\nu'\left(\boldsymbol{x}-\frac{\boldsymbol{r}}{2}\right)u_j'\left(\boldsymbol{x}+\frac{\boldsymbol{r}}{2}\right)\left[\rho'\left(\boldsymbol{x}+\frac{\boldsymbol{r}}{2}\right)-\rho'\left(\boldsymbol{x}-\frac{\boldsymbol{r}}{2}\right)\right]}\right)\bar{P}_{,i}(\boldsymbol{x})\tag{29}$$

$$\Gamma_3(\boldsymbol{x},\boldsymbol{r})=-\{b(\boldsymbol{x},0)a_j(\boldsymbol{x},-\boldsymbol{r})-b(\boldsymbol{x},\boldsymbol{r})a_j(\boldsymbol{x},0)\}\bar{P}_{,i}(\boldsymbol{x})\tag{30}$$

$$\Gamma_4(\boldsymbol{x},\boldsymbol{r})=\overline{\rho\left(\boldsymbol{x}+\frac{\boldsymbol{r}}{2}\right)u_j''\left(\boldsymbol{x}+\frac{\boldsymbol{r}}{2}\right)u_{i,n}''\left(\boldsymbol{x}-\frac{\boldsymbol{r}}{2}\right)}\left(\tilde{u}_n\left(\boldsymbol{x}+\frac{\boldsymbol{r}}{2}\right)-\tilde{u}_n\left(\boldsymbol{x}-\frac{\boldsymbol{r}}{2}\right)\right)\tag{31}$$

To obtain spectral forms, we Fourier transform two-point equation and take shell integrals in Fourier space. Assuming that the correlations are symmetric in r, e.g. $a_i(\boldsymbol{x},\boldsymbol{r})=a_i(\boldsymbol{x},-\boldsymbol{r})$, we obtain,

$$\begin{aligned}\frac{\partial\bar{\rho}(\boldsymbol{x})R_{ij}(\boldsymbol{x},k)}{\partial t}&+\left(\bar{\rho}(\boldsymbol{x})R_{ij}(\boldsymbol{x},k)\tilde{u}_n(\boldsymbol{x})\right)_{,n}\\&=\Gamma_{prod}(\boldsymbol{x},k)+\Gamma_{trans}(\boldsymbol{x},k)+\Gamma_{pstrain+diss}(\boldsymbol{x},k)+\sum_{i=1}^{4}\Gamma_i(\boldsymbol{x},k)\end{aligned}\tag{32}$$

The production term $\Gamma_{prod}(\boldsymbol{x},k)$ can be written,

$$\Gamma_{prod}(\boldsymbol{x},k)=-\bar{\rho}(\boldsymbol{x})R_{in}(\boldsymbol{x},k)\tilde{u}_{j,n}(\boldsymbol{x})-\bar{\rho}(\boldsymbol{x})R_{nj}(\boldsymbol{x},k)\tilde{u}_{i,n}(\boldsymbol{x})+\ a_i(\boldsymbol{x},k)\bar{P}_{,j}(\boldsymbol{x})+a_j(\boldsymbol{x},k)\bar{P}_{,i}(\boldsymbol{x})\tag{33}$$

The $\Gamma_3(\boldsymbol{x},k)$ term is modified to a symmetric form to ensure $R_{ij}(\boldsymbol{x},k)$ stays symmetric. The definition of $R_{ij}(\boldsymbol{x},k)$ is not guaranteed to stay symmetric, but it would require tracking an additional 3 components, and very similar forms of R_{ij} are symmetric.

$$\Gamma_3(\boldsymbol{x},k) = -\{b(\boldsymbol{x})a_j(\boldsymbol{x},k) - b(\boldsymbol{x},k)a_j(\boldsymbol{x})\}\bar{P}_{,i}(\boldsymbol{x}) \\ \approx -\frac{1}{2}\left[\{b(\boldsymbol{x})a_j(\boldsymbol{x},k) - b(\boldsymbol{x},k)a_j(\boldsymbol{x})\}\bar{P}_{,i}(\boldsymbol{x}) + \{b(\boldsymbol{x})a_i(\boldsymbol{x},k) - b(\boldsymbol{x},k)a_i(\boldsymbol{x})\}\bar{P}_{,j}(\boldsymbol{x})\right] \tag{34}$$

The transport term is modeled by a gradient diffusion argument in a similar manner as previous work [15],

$$\Gamma_{trans}(\boldsymbol{x},k) = C_d\left(\bar{\rho}(\boldsymbol{x})\nu_t(\boldsymbol{x})R_{ij,n}(\boldsymbol{x},k)\right)_{,n} \tag{35}$$

Where C_d is a tuned coefficient and the turbulent viscosity is taken to be uniform in k-space,

$$\nu_t(x) = \int_0^\infty \frac{\sqrt{kR_{nn}(x,k)}}{k^2}dk \tag{36}$$

The dissipation term is modeled by a k^2-type destruction proportional to the kinematic viscosity ν,

$$\Gamma_{diss}(\boldsymbol{x},k) = -2\nu k^2\bar{\rho}(\boldsymbol{x})R_{ij}(\boldsymbol{x},k) \tag{37}$$

In the same manner as BHR3.1 [3], the pressure strain term is modeled as a slow return-to-isotropy combined with a rapid distortion term,

$$\Gamma_{pstrain}(\boldsymbol{x},k) = \Gamma_{return-to-isotropy}(\boldsymbol{x},k) + \Gamma_{rapid\ distortion}(\boldsymbol{x},k) \tag{38}$$

$$\Gamma_{return-to-isotropy}(\boldsymbol{x},k) = -C_m\Theta^{-1}(\boldsymbol{x},k)\bar{\rho}(\boldsymbol{x})\left(R_{ij}(\boldsymbol{x},k) - \frac{\delta_{ij}}{3}R_{nn}(\boldsymbol{x},k)\right) \tag{39}$$

$$\Gamma_{rapid\ distortion}(\boldsymbol{x},k) \\ = -C_{r1}\{a_i(\boldsymbol{x},k)\bar{P}_{,j}(x) + a_j(\boldsymbol{x},k)\bar{P}_{,i}(\boldsymbol{x})\} \\ + C_{r2}\{\bar{\rho}(\boldsymbol{x})R_{in}(\boldsymbol{x},k)\tilde{u}_{j,n}(\boldsymbol{x}) + \bar{\rho}(\boldsymbol{x})R_{jn}(\boldsymbol{x},k)\tilde{u}_{i,n}(\boldsymbol{x})\} + \frac{2}{3}C_{r1}\bar{\rho}(\boldsymbol{x})a_k(\boldsymbol{x},k)\bar{P}_{,k}(\boldsymbol{x})\delta_{ij} \tag{40}$$

For now, the rapid distortion model and coefficient are taken directly from BHR3.1. The return to isotropy is taken to be proportional to the turbulent frequency [10],

$$\Theta^{-1}(\boldsymbol{x},k) = \int_0^k \sqrt{k'^2R_{nn}(\boldsymbol{x},k')}dk' \tag{41}$$

The $\Gamma_1(\boldsymbol{x},k)$ appears to represent the main cascade term, driving energy towards small wavenumbers. Here it is modeled by the the typical LWN cascade model with the addition of the backscatter term,

$$\Gamma_1(\boldsymbol{x},k) = \bar{\rho}(\boldsymbol{x})\frac{\partial}{\partial k}\left[k\left(\theta^{-1}(\boldsymbol{x},k) + \theta_{back}^{-1}(\boldsymbol{x},k)\right)\left[-C'_{r1}R_{ij}(\boldsymbol{x},k) + C'_{r2}k\frac{\partial R_{ij}(\boldsymbol{x},k)}{\partial k}\right]\right] \tag{42}$$

The $\Gamma_2(\boldsymbol{x},k)$ term is currently neglected.

The last $\Gamma_4(\boldsymbol{x},k)$ term representations distortion of the spectrum by the mean velocity field, such as bulk compression or expansion. This is currently modeled by a simple isotropic spectral-advection model for dilatation

$$\Gamma_4(\boldsymbol{x},k) = C_{comp}\bar{u}_{n,n}\frac{\partial}{\partial k}\left[kR_{ij}(\boldsymbol{x},k)\right] \tag{43}$$

2.5. $\boldsymbol{b}$ Equation

--- NOTE: The derivation used here for b isn't consistent with the derviations for a_i and R_{ij}. Use with caution. See Appendix A.3 for details.

To obtain a transport equation for $b(\boldsymbol{x},\boldsymbol{r})$, we multiple the transport equations forρ' and ν', evaluated at $x+\frac{r}{2}$ and $x-\frac{r}{2}$ respectively, [15]

$$\frac{\partial\rho'}{\partial t} + (\rho'\tilde{u}_n + \rho u''_n)_{,n} = 0 \tag{44}$$

$$\frac{\partial\nu'}{\partial t} + (\nu'\tilde{u}_n)_{,n} = 2\nu'(\tilde{u}_n)_{,n} + 2\left(\nu\, u''_{n,n} - \overline{\nu\, u''_{n,n}}\right) - (\nu u''_n - \overline{\nu u''_n})_{,n} \tag{45}$$

For the full derivation see Appendix A.3. Like in the $R_{ij}(x,r)$ transport equation, it is assumed that mean flow viscous stresses are neglible and mean flow quantities are approximatly uniform in r,

$$\frac{\partial \bar{\rho}(\boldsymbol{x}) b(\boldsymbol{x},\boldsymbol{r})}{\partial t} + \left(\bar{\rho}(\boldsymbol{x}) b(\boldsymbol{x},\boldsymbol{r}) \tilde{u}_n(\boldsymbol{x})\right)_{,n} = \bar{\rho}(\boldsymbol{x}) \left(\Gamma_{prod}(\boldsymbol{x},\boldsymbol{r}) + \Gamma_{redist}(\boldsymbol{x},\boldsymbol{r}) + \Gamma_{trans}(\boldsymbol{x},\boldsymbol{r}) + \Gamma_{decay}(\boldsymbol{x},\boldsymbol{r}) + \sum_{i=1}^{5} \Gamma_i(\boldsymbol{x},\boldsymbol{r}) \right) \tag{46}$$

The b-production term is,

$$\Gamma_{prod}(\boldsymbol{x},\boldsymbol{r}) = -\left(\frac{b(\boldsymbol{x})+1}{\bar{\rho}(\boldsymbol{x})}\right)\left(a_n(\boldsymbol{x},\boldsymbol{r}) + a_n(\boldsymbol{x},-\boldsymbol{r})\right) \bar{\rho}_{,n}(\boldsymbol{x}) \tag{47}$$

The b-redistribution term is,

$$\Gamma_{redist}(\boldsymbol{x},\boldsymbol{r}) = a_n(\boldsymbol{x},\boldsymbol{r}) b_{,n}(\boldsymbol{x}) + a_n(\boldsymbol{x}) b_{,n}(\boldsymbol{x},\boldsymbol{r}) \tag{48}$$

The b-transport term is,

$$\Gamma_{trans}(\boldsymbol{x},\boldsymbol{r}) = \bar{\rho}(\boldsymbol{x}) \left(\frac{\overline{\left(\nu'\left(\boldsymbol{x}-\frac{\boldsymbol{r}}{2}\right)\rho'\left(\boldsymbol{x}+\frac{\boldsymbol{r}}{2}\right)u_n'\left(\boldsymbol{x}-\frac{\boldsymbol{r}}{2}\right)\right)}}{\bar{\rho}(\boldsymbol{x})} \right)_{,n} \tag{49}$$

The b-decay term is,

$$\Gamma_{decay}(\boldsymbol{x},\boldsymbol{r}) = \bar{\rho}(\boldsymbol{x})\overline{\nu'\left(\boldsymbol{x}-\frac{\boldsymbol{r}}{2}\right)u_{n,n}''\left(\boldsymbol{x}+\frac{\boldsymbol{r}}{2}\right)} + \bar{\rho}(\boldsymbol{x})\overline{\nu'\left(\boldsymbol{x}+\frac{\boldsymbol{r}}{\boldsymbol{2}}\right)u_{n,n}''\left(\boldsymbol{x}-\frac{\boldsymbol{r}}{2}\right)} \tag{50}$$

The remaining terms are zero in the single point ($r=0$) case, $\Gamma_i(x,0)=0$

$$\Gamma_1(\boldsymbol{x},\boldsymbol{r}) = \overline{\left(\rho_{,n}'\left(\boldsymbol{x}+\frac{\boldsymbol{r}}{2}\right)\nu'\left(\boldsymbol{x}-\frac{\boldsymbol{r}}{2}\right)\right)\left(u_n'\left(\boldsymbol{x}+\frac{\boldsymbol{r}}{2}\right)-u_n'\left(\boldsymbol{x}-\frac{\boldsymbol{r}}{2}\right)\right)} \tag{51}$$

$$\Gamma_2(\boldsymbol{x},\boldsymbol{r}) = \overline{\rho'\left(\boldsymbol{x}+\frac{\boldsymbol{r}}{2}\right)\nu'\left(\boldsymbol{x}-\frac{\boldsymbol{r}}{2}\right)\left(u_{n,n}'\left(\boldsymbol{x}+\frac{\boldsymbol{r}}{2}\right)-u_{n,n}'\left(\boldsymbol{x}-\frac{\boldsymbol{r}}{2}\right)\right)} \tag{52}$$

$$\Gamma_3(\boldsymbol{x},\boldsymbol{r}) = \overline{\rho'\left(\boldsymbol{x}+\frac{\boldsymbol{r}}{2}\right)u_{n,n}'\left(\boldsymbol{x}-\frac{\boldsymbol{r}}{2}\right)\left(\nu'\left(\boldsymbol{x}+\frac{\boldsymbol{r}}{2}\right)-\nu'\left(\boldsymbol{x}-\frac{\boldsymbol{r}}{2}\right)\right)} \tag{53}$$

$$\Gamma_4(\boldsymbol{x},\boldsymbol{r}) = \frac{\bar{\rho}_{,n}(\boldsymbol{x})}{\bar{\rho}(\boldsymbol{x})}\left[\overline{\left(\nu'\left(\boldsymbol{x}-\frac{\boldsymbol{r}}{2}\right)\left(\rho'\left(\boldsymbol{x}+\frac{\boldsymbol{r}}{2}\right)u_n'\left(\boldsymbol{x}-\frac{\boldsymbol{r}}{2}\right)-\rho'\left(\boldsymbol{x}-\frac{\boldsymbol{r}}{2}\right)u_n'\left(\boldsymbol{x}+\frac{\boldsymbol{r}}{2}\right)\right)\right)}\right] \tag{54}$$

$$\Gamma_5(\boldsymbol{x},\boldsymbol{r}) = \bar{\rho}(\boldsymbol{x})\left[\frac{\left(\tilde{u}_n\left(\boldsymbol{x}+\frac{\boldsymbol{r}}{2}\right)-\tilde{u}_n\left(\boldsymbol{x}-\frac{\boldsymbol{r}}{2}\right)\right)}{2}\left(\overline{\rho_{,n}'\left(\boldsymbol{x}+\frac{\boldsymbol{r}}{2}\right)\nu'\left(\boldsymbol{x}-\frac{\boldsymbol{r}}{2}\right)}-\overline{\rho'\left(\boldsymbol{x}+\frac{\boldsymbol{r}}{2}\right)\nu_{,n}'\left(\boldsymbol{x}-\frac{\boldsymbol{r}}{2}\right)}\right)\right] \tag{55}$$

Like the R_{ij} equation, the b is transformed to Fourier space and shell integrated to give an equation for $b(\boldsymbol{x},k)$,

$$\frac{\partial \bar{\rho}(\boldsymbol{x}) b(\boldsymbol{x},k)}{\partial t} + \left(\bar{\rho}(\boldsymbol{x}) b(\boldsymbol{x},k) \tilde{u}_n(\boldsymbol{x})\right)_{,n} = \bar{\rho}(\boldsymbol{x}) \left(\Gamma_{prod}(\boldsymbol{x},k) + \Gamma_{redist}(\boldsymbol{x},k) + \Gamma_{trans}(\boldsymbol{x},k) + \Gamma_{decay}(\boldsymbol{x},k) + \sum_{i=1}^{4} \Gamma_i(\boldsymbol{x},k) \right) \tag{56}$$

The b-production term is,

$$\Gamma_{prod}(\boldsymbol{x},k) = -2\left(\frac{b(\boldsymbol{x})+1}{\bar{\rho}(\boldsymbol{x})}\right) a_n(\boldsymbol{x},k)\, \bar{\rho}_{,n}(\boldsymbol{x}) \tag{57}$$

The b-redistribution term is,

$$\Gamma_{redist}(\boldsymbol{x},k) = a_n(\boldsymbol{x},k) b_{,n}(\boldsymbol{x}) + a_n(\boldsymbol{x}) b_{,n}(\boldsymbol{x},k) \tag{58}$$

The b-transport term is modeled by a gradient diffusion approximation analogous to BHR3.1 [3],

$$\Gamma_{trans}(\boldsymbol{x},k) = C_d\bar{\rho}(\boldsymbol{x})^2\left(\frac{\nu_t(\boldsymbol{x})b_{,n}(\boldsymbol{x},k)}{\bar{\rho}(\boldsymbol{x})}\right)_{,n} \tag{59}$$

The b-decay term is modeled as,

$$\Gamma_{decay}(\boldsymbol{x},k) = -2\nu k^2\bar{\rho}(\boldsymbol{x})b(\boldsymbol{x},k) \tag{60}$$

The predominant cascade term is modeled as

$$\Gamma_1(\boldsymbol{x},k) = \bar{\rho}(\boldsymbol{x})\frac{\partial}{\partial k}\left[k\left(\theta^{-1}(\boldsymbol{x},k)+\theta_{back}^{-1}(\boldsymbol{x},k)\right)\left[-C'_{b1}b(\boldsymbol{x},k)+C'_{b2}k\frac{\partial b(\boldsymbol{x},k)}{\partial k}\right]\right] \tag{61}$$

The remaining terms, $\Gamma_2(\boldsymbol{x},k)$, $\Gamma_3(\boldsymbol{x},k)$, and $\Gamma_4(\boldsymbol{x},k)$, are neglected.

The compression term is modeled in the same manner as R_{ij}, $\Gamma_5(\boldsymbol{x},k) = C_{comp}\bar{u}_{n,n}\frac{\partial}{\partial k}[kb(\boldsymbol{x},k)]$

2.6. $\boldsymbol{a_i}$ Equation

To obtain a transport equation for $a_i(\boldsymbol{x},\boldsymbol{r})$, we multiple the transport equations forρ' and u'', evaluated at $x+\frac{r}{2}$ and $x-\frac{r}{2}$ respectively, [15]

$$\frac{\partial\rho'}{\partial t}+(\rho'\tilde{u}_n+\rho u_n'')_{,n}=0 \tag{62}$$

$$\frac{\partial u_i''}{\partial t}+u_n''(\tilde{u}_i+u_i'')_{,n}+\tilde{u}_n u_{i,n}''=\left(\bar{v}-\frac{1}{\bar{\rho}}\right)\bar{\sigma}_{ni,n}+v'\bar{\sigma}_{ni,n}+v\sigma_{ni,n}'+\frac{1}{\bar{\rho}}(\bar{\rho}R_{ni})_{,n} \tag{63}$$

See Appendix A.2 for a derivation. Making the same assumptions used to simplify the $R_{ij}(x,r)$ transport equation, with the additional assumption that $u_{n,n}'\approx 0$, as done in the a_i equation in BHR3 [4], yields,

$$\begin{aligned}\frac{\partial\bar{\rho}(\boldsymbol{x})a_i(\boldsymbol{x},\boldsymbol{r})}{\partial t}&+\left(\bar{\rho}(\boldsymbol{x})a_i(\boldsymbol{x},\boldsymbol{r})\tilde{u}_n(\boldsymbol{x})\right)_{,n}\\&=\Gamma_{prod}(\boldsymbol{x},\boldsymbol{r})+\Gamma_{redist}(\boldsymbol{x},\boldsymbol{r})+\Gamma_{trans}(\boldsymbol{x},\boldsymbol{r})+\Gamma_{drag}(\boldsymbol{x},\boldsymbol{r})+\Gamma_{decay}(\boldsymbol{x},\boldsymbol{r})\\&+\sum_{i=1}^{4}\Gamma_i(\boldsymbol{x},k)\end{aligned} \tag{64}$$

The production term is,

$$\Gamma_{prod}(\boldsymbol{x},\boldsymbol{r})=b(\boldsymbol{x},\boldsymbol{r})\bar{P}_{,i}(\boldsymbol{x})-R_{in}(\boldsymbol{x},\boldsymbol{r})\bar{\rho}_{,n}(\boldsymbol{x})-\bar{\rho}(x)a_i(\boldsymbol{x},\boldsymbol{r})\bar{u}_{i,n}(\boldsymbol{x}) \tag{65}$$

The redistribution term is,

$$\Gamma_{redist}(\boldsymbol{x},\boldsymbol{r})=\bar{\rho}(\boldsymbol{x})\big(a_i(\boldsymbol{x},\boldsymbol{r})a_n(\boldsymbol{x})\big)_{,n} \tag{66}$$

The transport term is,

$$\Gamma_{trans}(\boldsymbol{x},\boldsymbol{r})=-\bar{\rho}(x)\left(\frac{\overline{\rho'\left(\boldsymbol{x}+\frac{\boldsymbol{r}}{2}\right)u_i'\left(\boldsymbol{x}-\frac{\boldsymbol{r}}{2}\right)u_n'\left(\boldsymbol{x}+\frac{\boldsymbol{r}}{2}\right)}}{\bar{\rho}(\boldsymbol{x})}\right)_{,n} \tag{67}$$

The pressure drag term is,

$$\Gamma_{drag}(\boldsymbol{x},\boldsymbol{r})=\bar{\rho}(x)\overline{v'\left(x+\frac{\boldsymbol{r}}{2}\right)p_{,i}'\left(x-\frac{\boldsymbol{r}}{2}\right)} \tag{68}$$

The viscous decay term is,

$$\Gamma_{decay}(\boldsymbol{x},\boldsymbol{r})=-\bar{\rho}(x)\overline{v'\left(x+\frac{\boldsymbol{r}}{2}\right)\tau_{ni,n}'\left(x-\frac{\boldsymbol{r}}{2}\right)} \tag{69}$$

The remaining terms have $\Gamma_i(x,0)=0$, and are

$$\Gamma_1(\boldsymbol{x},\boldsymbol{r})=\overline{\rho'\left(\boldsymbol{x}+\frac{\boldsymbol{r}}{2}\right)u_{i,n}'\left(\boldsymbol{x}-\frac{\boldsymbol{r}}{2}\right)\left[u_n''\left(\boldsymbol{x}+\frac{\boldsymbol{r}}{2}\right)-u_n''\left(\boldsymbol{x}-\frac{\boldsymbol{r}}{2}\right)\right]} \tag{70}$$

$$\Gamma_2(\boldsymbol{x},\boldsymbol{r})=\overline{\rho'\left(\boldsymbol{x}+\frac{\boldsymbol{r}}{2}\right)\tau_{ni,n}'\left(\boldsymbol{x}-\frac{\boldsymbol{r}}{2}\right)\left(v'\left(\boldsymbol{x}-\frac{\boldsymbol{r}}{2}\right)-v'\left(\boldsymbol{x}+\frac{\boldsymbol{r}}{2}\right)\right)} \tag{71}$$

$$\Gamma_3(\boldsymbol{x},\boldsymbol{r})=\overline{\rho'\left(\boldsymbol{x}+\frac{\boldsymbol{r}}{2}\right)p_{,i}'\left(\boldsymbol{x}-\frac{\boldsymbol{r}}{2}\right)\left(v'\left(\boldsymbol{x}+\frac{\boldsymbol{r}}{2}\right)-v'\left(\boldsymbol{x}-\frac{\boldsymbol{r}}{2}\right)\right)} \tag{72}$$

$$\Gamma_4(\boldsymbol{x},\boldsymbol{r})=\overline{\rho'\left(\boldsymbol{x}+\frac{\boldsymbol{r}}{2}\right)u_{i,n}''\left(\boldsymbol{x}-\frac{\boldsymbol{r}}{2}\right)}\left(\tilde{u}_n\left(\boldsymbol{x}+\frac{\boldsymbol{r}}{2}\right)-\tilde{u}_n\left(\boldsymbol{x}-\frac{\boldsymbol{r}}{2}\right)\right) \tag{73}$$

Fourier transforming and shell integrating yields,

$$\begin{aligned}\frac{\partial\bar{\rho}(\boldsymbol{x})a_i(\boldsymbol{x},k)}{\partial t} &+ \left(\bar{\rho}(\boldsymbol{x})a_i(\boldsymbol{x},k)\tilde{u}_n(\boldsymbol{x})\right)_{,n} \\ &= \Gamma_{prod}(\boldsymbol{x},k) + \Gamma_{redist}(\boldsymbol{x},k) + \Gamma_{trans}(\boldsymbol{x},k) + \Gamma_{drag}(\boldsymbol{x},k) + \Gamma_{decay}(\boldsymbol{x},k) \\ &+ \sum_{i=1}^{4}\Gamma_i(\boldsymbol{x},k)\end{aligned} \tag{74}$$

The production term is,

$$\Gamma_{prod}(\boldsymbol{x},k) = b(\boldsymbol{x},k)\bar{P}_{,i}(\boldsymbol{x}) - R_{in}(\boldsymbol{x},k)\bar{\rho}_{,n}(\boldsymbol{x}) - \bar{\rho}(x)a_i(\boldsymbol{x},k)\bar{u}_{i,n}(\boldsymbol{x}) \tag{75}$$

The redistribution term is,

$$\Gamma_{redist}(\boldsymbol{x},k) = \bar{\rho}(\boldsymbol{x})\left(a_i(\boldsymbol{x},k)a_n(\boldsymbol{x})\right)_{,n} \tag{76}$$

The transport term is modeled by gradient diffusion,

$$\Gamma_{trans}(\boldsymbol{x},k) = C_d\bar{\rho}(\boldsymbol{x})\left(\nu_t(\boldsymbol{x})a_{i,n}(\boldsymbol{x},k)\right)_{,n} \tag{77}$$

The drag term is modeled in the same manner as previous LWN approaches [1, 10], (no summation over α), plus the rapid decay term used in BHR3.1 [3]

$$\begin{aligned}\Gamma_{drag}(\boldsymbol{x},k) = -&\left[C_{rp1}k^2|a_\alpha(\boldsymbol{x},k)| + C_{rp2}\Theta^{-1}(\boldsymbol{x},k)\right]a_\alpha(\boldsymbol{x},k)\delta_{i\alpha} - C_{ap}\,b(\boldsymbol{x},k)\bar{P}_{,i}(\boldsymbol{x}) \\ &+ C_{au}\bar{\rho}(\boldsymbol{x})a_k(\boldsymbol{x},k)\bar{u}_{i,k}(\boldsymbol{x})\end{aligned} \tag{78}$$

The a_i-decay term is modeled as,

$$\Gamma_{decay}(\boldsymbol{x},k) = -2\nu k^2\bar{\rho}(\boldsymbol{x})a_i(\boldsymbol{x},k) \tag{79}$$

The predominant cascade term is modeled as

$$\Gamma_1(\boldsymbol{x},k) = \bar{\rho}(\boldsymbol{x})\frac{\partial}{\partial k}\left[k\left(\theta^{-1}(\boldsymbol{x},k) + \theta_{back}^{-1}(\boldsymbol{x},k)\right)\left[-C'_{a1}a_i(\boldsymbol{x},k) + C'_{a2}k\frac{\partial a_i(\boldsymbol{x},k)}{\partial k}\right]\right] \tag{80}$$

The terms $\Gamma_2(\boldsymbol{x},k)$ and $\Gamma_3(\boldsymbol{x},k)$ are currently neglected

The compression term is modeled analogously to the R_{ij} compression,

$$\Gamma_4(\boldsymbol{x},k) = C_{comp}\bar{u}_{n,n}\frac{\partial}{\partial k}\left[ka_i(\boldsymbol{x},k)\right] \tag{81}$$

2.7. Model Summary

The model is summarized below. While there was previously a lot of derivation, not much is different from the current implementation of LWN in xRage. Terms that are different from the current LWN xRage implementation are highlighted in blue.

$\frac{\partial\bar{\rho}}{\partial t} + \left(\bar{\rho}\tilde{u}_j\right)_{,j} = 0,$	(82)
$\frac{\partial\bar{\rho}\tilde{u}_i}{\partial t} + \left(\bar{\rho}\tilde{u}_i\tilde{u}_j + P\delta_{ij} + \bar{\rho}\tilde{R}_{ij}\right)_{,j} = \bar{\rho}g$	(83)
$\frac{\partial\bar{\rho}\tilde{E}}{\partial t} + \left(\bar{\rho}\tilde{E}\tilde{u}_j + P\tilde{u}_j + \bar{\rho}\tilde{u}_i\tilde{R}_{ij} - \bar{\rho}\sum_k h^k a_j^k\right)_{,j} = C_d\left(\bar{\rho}\nu_t\left(K_{,j} + C_v T_{,j}\right)\right)_{,j}$	(84)
$\frac{\partial\bar{\rho}\tilde{c}^k}{\partial t} + \left(\bar{\rho}\tilde{u}_j\tilde{c}^k - \bar{\rho}a_j^k\right)_{,j} = 0$	(85)
$\frac{\partial\bar{\rho}(\boldsymbol{x})R_{ij}(\boldsymbol{x},k)}{\partial t} + \left(\bar{\rho}(\boldsymbol{x})R_{ij}(\boldsymbol{x},k)\tilde{u}_n(\boldsymbol{x})\right)_{,n} = \Gamma_{prod}(\boldsymbol{x},k) + \Gamma_{trans}(\boldsymbol{x},k) + \Gamma_{diss}(\boldsymbol{x},k) + \Gamma_{return-to-isotropy}(\boldsymbol{x},k) + \Gamma_{rapid\ distortion}(\boldsymbol{x},k) + \Gamma_1(\boldsymbol{x},k) + \Gamma_3(\boldsymbol{x},k) + \Gamma_4(\boldsymbol{x},k)$ $\Gamma_{prod}(\boldsymbol{x},k) = -\bar{\rho}(\boldsymbol{x})R_{in}(\boldsymbol{x},k)\tilde{u}_{j,n}(\boldsymbol{x}) - \bar{\rho}(\boldsymbol{x})R_{nj}(\boldsymbol{x},k)\tilde{u}_{i,n}(\boldsymbol{x}) + a_i(\boldsymbol{x},k)\bar{P}_{,j}(\boldsymbol{x}) + a_j(\boldsymbol{x},k)\bar{P}_{,i}(\boldsymbol{x})$ $\Gamma_{trans}(\boldsymbol{x},k) = C_d\left(\bar{\rho}(\boldsymbol{x})\nu_t(\boldsymbol{x})R_{ij,n}(\boldsymbol{x},k)\right)_{,n}$ $\Gamma_{diss}(\boldsymbol{x},k) = -2\nu k^2\bar{\rho}(\boldsymbol{x})R_{ij}(\boldsymbol{x},k)$ $\Gamma_{return-to-isotropy}(\boldsymbol{x},k) = -C_m\Theta^{-1}(\boldsymbol{x},k)\bar{\rho}(\boldsymbol{x})\left(R_{ij}(\boldsymbol{x},k) - \frac{\delta_{ij}}{3}R_{nn}(\boldsymbol{x},k)\right)$ $\Gamma_{rapid\ distortion}(\boldsymbol{x},k) = -C_{r1}\left\{a_i(\boldsymbol{x},k)\bar{P}_{,j}(\boldsymbol{x}) + a_j(\boldsymbol{x},k)\bar{P}_{,i}(\boldsymbol{x})\right\} + C_{r2}\left\{\bar{\rho}(\boldsymbol{x})R_{in}(\boldsymbol{x},k)\tilde{u}_{j,n}(\boldsymbol{x}) + \bar{\rho}(\boldsymbol{x})R_{jn}(\boldsymbol{x},k)\tilde{u}_{i,n}(\boldsymbol{x})\right\} + \frac{2}{3}C_{r1}\bar{\rho}(\boldsymbol{x})a_k(\boldsymbol{x},k)\bar{P}_{,k}(\boldsymbol{x})\delta_{ij} - \frac{2}{3}C_{r2}\bar{\rho}R_{mk}(\boldsymbol{x},k)\tilde{u}_{m,k}\delta_{ij}$ $\Gamma_1(\boldsymbol{x},k) = \bar{\rho}(\boldsymbol{x})\frac{\partial}{\partial k}\left[k\left(\theta^{-1}(\boldsymbol{x},k) + \theta_{back}^{-1}(\boldsymbol{x},k)\right)\left[-C'_{r1}R_{ij}(\boldsymbol{x},k) + C'_{r2}k\frac{\partial R_{ij}(\boldsymbol{x},k)}{\partial k}\right]\right]$ $\Gamma_3(\boldsymbol{x},k) = -\frac{1}{2}\{b(\boldsymbol{x})a_j(\boldsymbol{x},k) - b(\boldsymbol{x},k)a_j(\boldsymbol{x})\}\bar{P}_{,i}(\boldsymbol{x}) - \frac{1}{2}\{b(\boldsymbol{x})a_i(\boldsymbol{x},k) - b(\boldsymbol{x},k)a_i(\boldsymbol{x})\}\bar{P}_{,j}(\boldsymbol{x})$ $\Gamma_4(\boldsymbol{x},k) = C_{comp}\bar{u}_{n,n}\frac{\partial}{\partial k}\left[kR_{ij}(\boldsymbol{x},k)\right]$	(86)

$\begin{gathered} \frac{\partial \bar{\rho}(\boldsymbol{x}) b(\boldsymbol{x},k)}{\partial t} + \left(\bar{\rho}(\boldsymbol{x}) b(\boldsymbol{x},k) \tilde{u}_n(\boldsymbol{x})\right)_{,n} = \bar{\rho}(\boldsymbol{x}) \left(\Gamma_{prod}(\boldsymbol{x},k) + \Gamma_{redist}(\boldsymbol{x},k) + \Gamma_{trans}(\boldsymbol{x},k) + \Gamma_{drag}(\boldsymbol{x},k) + \Gamma_{decay}(\boldsymbol{x},k) + \Gamma_1(\boldsymbol{x},k) + \Gamma_5(\boldsymbol{x},k)\right) \\ \Gamma_{prod}(\boldsymbol{x},k) = -2\left(\frac{b(\boldsymbol{x})+1}{\bar{\rho}(\boldsymbol{x})}\right) a_n(\boldsymbol{x},k)\, \bar{\rho}_{,n}(\boldsymbol{x}) \\ \Gamma_{redist}(\boldsymbol{x},k) = a_n(\boldsymbol{x},k) b_{,n}(\boldsymbol{x}) + a_n(\boldsymbol{x}) b_{,n}(\boldsymbol{x},k) \\ \Gamma_{trans}(\boldsymbol{x},k) = C_d \bar{\rho}(\boldsymbol{x}) \left(\nu_t(\boldsymbol{x}) b_{,n}(\boldsymbol{x},k)\right)_{,n} \\ \Gamma_{decay}(\boldsymbol{x},k) = -2\nu k^2 \bar{\rho}(\boldsymbol{x}) b(\boldsymbol{x},k) \\ \Gamma_1(\boldsymbol{x},k) = \bar{\rho}(x) \frac{\partial}{\partial k}\left[k\left(\theta^{-1}(\boldsymbol{x},k) + \theta_{back}^{-1}(\boldsymbol{x},k)\right)\left[-C'_{b1} b(\boldsymbol{x},k) + C'_{b2} k \frac{\partial b(\boldsymbol{x},k)}{\partial k}\right]\right] \\ \Gamma_5(\boldsymbol{x},k) = C_{comp} \bar{u}_{n,n} \frac{\partial}{\partial k}[k b(\boldsymbol{x},k)] \end{gathered}$	(87)
$\begin{gathered} \frac{\partial \bar{\rho}(\boldsymbol{x}) a_i(\boldsymbol{x},k)}{\partial t} + \left(\bar{\rho}(\boldsymbol{x}) a_i(\boldsymbol{x},k) \tilde{u}_n(\boldsymbol{x})\right)_{,n} = \Gamma_{prod}(\boldsymbol{x},k) + \Gamma_{redist}(\boldsymbol{x},k) + \Gamma_{trans}(\boldsymbol{x},k) + \Gamma_{decay}(\boldsymbol{x},k) + \Gamma_1(\boldsymbol{x},k) + \Gamma_4(\boldsymbol{x},k) \\ \Gamma_{prod}(\boldsymbol{x},k) = b(\boldsymbol{x},k) \bar{P}_{,i}(\boldsymbol{x}) - R_{in}(\boldsymbol{x},k) \bar{\rho}_{,n}(\boldsymbol{x}) - \bar{\rho}(x) a_i(\boldsymbol{x},k) \bar{u}_{i,n}(\boldsymbol{x}) \\ \Gamma_{redist}(\boldsymbol{x},k) = C_{a3} \bar{\rho}(\boldsymbol{x}) \left(a_i(\boldsymbol{x},k) a_n(\boldsymbol{x})\right)_{,n} \\ \Gamma_{trans}(\boldsymbol{x},k) = C_d \bar{\rho}(\boldsymbol{x}) \left(\nu_t(\boldsymbol{x}) a_{i,n}(\boldsymbol{x},k)\right)_{,n} \\ \Gamma_{drag}(\boldsymbol{x},k) = -\left[C_{rp1} k^2 \lvert a_\alpha(\boldsymbol{x},k)\rvert + C_{rp2} \Theta^{-1}(\boldsymbol{x},k)\right] a_\alpha(\boldsymbol{x},k) \delta_{i\alpha} - C_{ap}\, b(\boldsymbol{x},k) \bar{P}_{,i}(\boldsymbol{x}) + C_{au} \bar{\rho}(\boldsymbol{x}) a_k(\boldsymbol{x},k) \bar{u}_{i,k}(\boldsymbol{x}) \\ \Gamma_{decay}(\boldsymbol{x},k) = -2\nu k^2 \bar{\rho}(\boldsymbol{x}) a_i(\boldsymbol{x},k) \\ \Gamma_1(\boldsymbol{x},k) = \bar{\rho}(x) \frac{\partial}{\partial k}\left[k\left(\theta^{-1}(\boldsymbol{x},k) + \theta_{back}^{-1}(\boldsymbol{x},k)\right)\left[-C'_{a1} a_i(\boldsymbol{x},k) + C'_{a2} k \frac{\partial a_i(\boldsymbol{x},k)}{\partial k}\right]\right] \\ \Gamma_4(\boldsymbol{x},k) = C_{comp} \bar{u}_{n,n} \frac{\partial}{\partial k}[k a_i(\boldsymbol{x},k)] \end{gathered}$	(88)
$\begin{gathered} \frac{\partial \bar{\rho}(\boldsymbol{x}) a_i^k(\boldsymbol{x})}{\partial t} + \left(\bar{\rho}(\boldsymbol{x}) \tilde{u}_j(\boldsymbol{x}) a_i^k(\boldsymbol{x})\right)_{,j} \\ = (1 - C_{ap}) b^k(\boldsymbol{x}) \bar{P}_{,i}(\boldsymbol{x}) + \bar{\rho}(\boldsymbol{x}) \tilde{R}_{ij}(\boldsymbol{x}) \tilde{c}^k_{,j} - (1 - C_{au}) \bar{\rho}(\boldsymbol{x}) a_j^k(\boldsymbol{x}) \bar{u}_{i,j}(\boldsymbol{x}) + a_i(\boldsymbol{x}) \left(\bar{\rho}(\boldsymbol{x}) a_j^k(\boldsymbol{x})\right)_{,j} + C_d \bar{\rho}(\boldsymbol{x}) \left(\nu_t(\boldsymbol{x}) a_i^k(\boldsymbol{x})\right)_{,n} - a_j^k(x) \frac{\varepsilon_a}{a_j(\boldsymbol{x})} \end{gathered}$	(89)
$\frac{\partial \bar{\rho}(\boldsymbol{x}) b^k(\boldsymbol{x})}{\partial t} + \left(\bar{\rho}(\boldsymbol{x}) \tilde{u}_j(\boldsymbol{x}) b^k(\boldsymbol{x})\right)_{,j} = \bar{\rho} a_j(\boldsymbol{x}) \left(\tilde{c}^k(\boldsymbol{x}) + 2 b^k(\boldsymbol{x})\right)_{,j} + \bar{\rho}(\boldsymbol{x}) b^k(\boldsymbol{x}) a_{j,j}(\boldsymbol{x}) - a_j^k(\boldsymbol{x}) \bar{\rho}_{,j}(\boldsymbol{x}) + C_d \bar{\rho}(\boldsymbol{x}) \left(\nu_t(\boldsymbol{x}) b^k(\boldsymbol{x})\right)_{,n} - b^k(\boldsymbol{x}) \frac{\varepsilon_b}{b(\boldsymbol{x})}$	(90)

$$
\begin{aligned}
\Theta^{-1}(\boldsymbol{x},k) &= \int_0^k \sqrt{k'^2 R_{nn}(\boldsymbol{x},k')}\,dk' \\
\theta_{back}^{-1}(\boldsymbol{x},k) &= (L_I)^{-\frac{17}{2}} \int_k^\infty \sqrt{(k')^{-15} R_{nn}(\boldsymbol{x},k')}\,dk' \\
L_I &= \frac{3\pi}{4} \frac{\int_0^\infty k^{-1} R_{nn}(\boldsymbol{x},k)dk}{\int_0^\infty R_{nn}(\boldsymbol{x},k)dk} \\
v_t(x) &= \int_0^\infty \frac{\sqrt{kR_{nn}(x,k)}}{k^2}\,dk
\end{aligned} \tag{91}
$$

2.8. Coefficients

The coefficients are set roughly against matching RT and HRT simulations or based on their value from BHR3.1. Tuning will be required, particularly in cases where the values are unchanged from BHR3.1.

Coefficient	Value	Equation	Role
C_d	2.0	all	Turbulent diffusion
C_m	1.0	R_{ij}	Slow return to isotropy
C_{r1}	0.3	R_{ij}	Rapid return to isotropy
C_{r2}	0.3	R_{ij}	Rapid return to isotropy
C'_{r1}	0.24	R_{ij}	Leith advection in k-space
C'_{r2}	0.06	R_{ij}	Leith diffusion in k-space
C'_{b1}	0.24	b	Leith advection in k-space
C'_{b2}	0.06	b	Leith diffusion in k-space
C_{ap}	0.2	a_i	Rapid decay
C_{au}	0.4	a_i	Rapid decay
C'_{a1}	0.24	a_i	Leith advection in k-space
C'_{a2}	0.06	a_i	Leith diffusion in k-space
C_{rp1}	0.	a_i	Pressure drag
C_{rp2}	0.2	a_i	Pressure drag
C_{a3}	0	a_i	Flag for swapping between a_i-transport closures
C_{comp}	1/3	all	Spectral compression by velocity dilatation

2.8.1. Cascade coefficients

The Kolmogorov coefficient consistent with the R_{ij} cascade coefficients can be calculated in the same manner as in [14]. Neglecting the backscatter term, which decays rapidly at high wavenumbers, the cascade of turbulent kinetic energy, $K = \frac{1}{2}R_{ii}$, is

$$F(\boldsymbol{x},k) = \frac{1}{2}\left[k\,\theta^{-1}(\boldsymbol{x},k)\left[-C'_{r1}R_{ii}(\boldsymbol{x},k) + C'_{r2}k\frac{\partial R_{ii}(\boldsymbol{x},k)}{\partial k}\right]\right] \tag{92}$$

Assuming an inertial range spectrum of the form $R_{ii} = 2K_0k^{-\frac{5}{3}}$,

$$\theta^{-1}(\boldsymbol{x},k) = \int_0^k \sqrt{k'^2R_{ii}(\boldsymbol{x},k')}dk' = \sqrt{\frac{3k^{\frac{4}{3}}K_0}{2}} \tag{93}$$

$$F(\boldsymbol{x},k) = \frac{\sqrt{6}}{2}K_0^{\frac{3}{2}}\left[-C'_{r1} - \frac{5}{3}C'_{r2}\right] \tag{94}$$

The dissipation of K, ε, must equal the negative of the flux of K in a steady state inertial range. For a Kolmogorov spectrum $E(k) = C_K\varepsilon^{\frac{2}{3}}k^{-\frac{5}{3}}$,

$$C_K = E(k)(-F)^{-\frac{2}{3}}k^{\frac{5}{3}} = \left(\frac{\sqrt{6}}{2}\left[C'_{r1} + \frac{5}{3}C'_{r2}\right]\right)^{-\frac{2}{3}} \tag{95}$$

This gives a relation for the advection coefficient,

$$C'_{r1} = \sqrt{\frac{2}{3}}C_K^{-\frac{3}{2}} - \frac{5}{3}C'_{r2} \tag{96}$$

Additionally, the requirement that the backscatter term vanishes in a k^4 spectrum requires $C'_{r1} = 4C'_{r2}$. Experimental data suggests $C_K \approx 1.5$ [23] while recent DNS has found a value closer to $C_K \approx 1.8$ [24]. Taking $C_K \approx 1.8$, these two requirements give

$$C'_{r1} = \frac{4\sqrt{6}}{17} C_K^{-\frac{3}{2}} \approx 0.24 \tag{97}$$

$$C'_{r2} = \frac{C'_{r1}}{4} \approx 0.06 \tag{98}$$

The cascade terms for a_i and b may be empirically tuned, but still require $C'_{a1} = 4C'_{a2}$ and $C'_{b1} = 4C'_{b2}$ to fulfill the requirements of the backscatter term vanishing at the lower k-space boundary.

3. Reconstruct Evolve Average (REA)

Numerical error in PDE's is typically dominated by the ability to reconstruct derivatives, and derivatives in LWN are mostly separated between physical space derivatives $\partial/\partial x_i$ and spectral derivatives $\partial/\partial k$. The most numerically expensive operations in LWN are typically associated with the spatial derivatives, as operations such as diffusion in x are global and highly costly, and must be done for every wavenumber tracked in LWN. As a result, tracking a large number of wavenumbers in LWN is expensive due to the physical space updates, even though the impact on accuracy of tracking many wavenumbers is largely relevant only to the spectral updates due to the presence of $\partial/\partial k$ derivatives. This creates a situation where there is substantial incentive to find high-accuracy methods to solve the k-space updates even if these higher accuracy methods are relatively costly, because these would allow us to track fewer wavenumbers and thus reduce the cost of the much more expensive physical space updates.

High order methods were tried but it appears that methods applied to the k-space updates should be monotone for stability reasons – a property rarely present in high order methods. One option for at least approaching this issue is to use Reconstruct-Evolve-Average (REA) methods, which are time-stepped with the following procedure:

- Reconstruct the coarse-grid function with an interpolating function that is evaluated on the much finer grid. The interpolation must have the property that it averages across each grid cell to equal the cell center value of the original coarse grid function.
- Evolve the interpolating function to get the next timestep of the fine grid solution using any appropriate finite-volume scheme. Normally REA schemes do not explicitly solve the interpolating function on a fine grid (instead using analytical methods to calculate fluxes) but to the authors' knowledge one needs to explicitly update it on a grid when doing updates in k-space implicitly in time.
- Average the fine grid interpolating function to return to the original coarse grid solution.

REA methods are particularly appealing because it is easy to enforce monotonicity by using upwind schemes on the fine grid update step, and we know the solutions we are looking for in k-space look like power laws. We can thus use power law interpolation schemes to reconstruct the fine grid interpolation, and should be able to expect a high degree of accuracy in that interpolation even when using few coarse grid points.

3.1. REA interpolation

The main choice in REA is how to interpolate the function during each k-space update. The most obvious choice is some form of power law interpolation. A basic schematic for the interpolation is below,

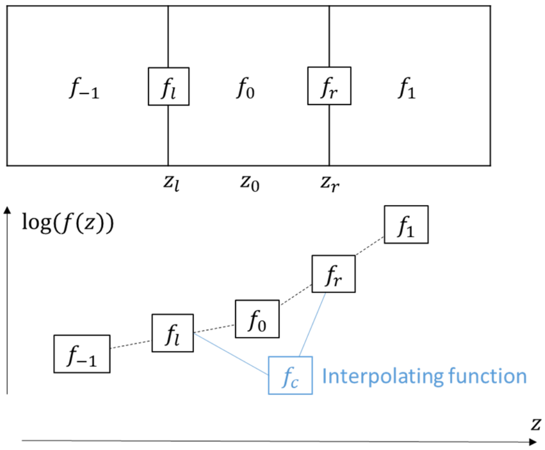

Figure 3 Schematic for the REA interpolation approach. The cell centered values of f on the grid in z are f_{-1}, f_0, f_1, where f_0 is in the cell we are currently interplating across. The cell-face powerlaw interpolations are f_l and f_r, griven by equation (99), and z_l and z_r are the location in z of the left and right cell face. The interpolating function is defined by a power law interpolation to a point at $z = z_c$ and $f = f_c$.

In all cases we assumed $f(k) = kg(k)$, where $g(k)$ is the function we're evolving in LWN, e.g. $R_{ij}(x,k)$, so that we can integrate $f(z)$ on a uniform grid in z. The value f_0 is the cell average (or cell-centered value) of the function in the cell we're currently interpolating across. The cell averages of the cells to the left and right are f_{-1} and f_1 respectively. Assuming f varies as a power-law, i.e. $f(k) \propto k^n$, and assuming a uniform grid spacing in z, $z = \log\left(\frac{k}{k_0}\right)$, then the face centered values interpolate to,

$$f_l = \sqrt{f_{-1} f_0}; \qquad f_r = \sqrt{f_0 f_1} \tag{99}$$

We then look for a solution interpolating between these face values and some central point (z_c, f_c),

$$f_{int}(z) = \begin{cases} f_c \left(\frac{f_l}{f_c}\right)^{\frac{z_c - z}{z_c - z_l}} & z < z_c \\ f_c \left(\frac{f_r}{f_c}\right)^{\frac{z - z_c}{z_r - z_c}} & z > z_c \end{cases} \tag{100}$$

For the average of the function to equal the original cell average, we must have

$$\frac{1}{(z_r - z_l)} \int_{z_l}^{z_r} f_{int}(z)\, dz = f_0 \tag{101}$$

To fulfill this for the assumed form of the interpolating function (100), we must fulfill

$$0 = \frac{\left[f_0 (z_r - z_l) \log\left(\frac{f_r}{f_c}\right) + z_r (f_c - f_r)\right] \log\left(\frac{f_l}{f_c}\right) - z_l \log\left(\frac{f_r}{f_c}\right)(f_c - f_l)}{(f_c - f_r)\log\left(\frac{f_l}{f_c}\right) - (f_c - f_l)\log\left(\frac{f_r}{f_c}\right)} - z_c \tag{102}$$

One option is to set $f_c = f_0$ and vary z_c, which is easily solved for. However, this was found to have mediocre results in practice, and one must handle how z_c behaves if it falls outside the cell.

The other obvious option is to set $z_c = z_0$ and vary f_c until the interpolating function integrates to the correct value. Unfortunately we do not have an analytical solution to the above equation for f_c, so instead we use Newton's method to approximate it. Because we may be searching for solutions extremely close to zero, we use a regularized form that prevents f_c from changing sign,

$$f_c^* = \begin{cases} f_c - F\dfrac{\partial F}{\partial f_c} & if \quad \dfrac{f_c}{F}\dfrac{\partial F}{\partial f_c} < 0 \\ f_c - F\left(\dfrac{f_c^*}{f_c}\right)\dfrac{\partial F}{\partial f_c} & if \quad \dfrac{f_c}{F}\dfrac{\partial F}{\partial f_c} > 0 \end{cases} \tag{103}$$

Where f_c^* is the value of f_c at the end of one iteration, and F is the error in the evaluated integral relative to the original cell average in (101) ,

$$F = \left(\frac{(z_c - z_r)(f_c - f_r)}{\log\left(\frac{f_r}{f_c}\right)} - \frac{(z_c - z_l)(f_c - f_l)}{\log\left(\frac{f_l}{f_c}\right)}\right) - \frac{f_0}{(z_r - z_l)} \tag{104}$$

$$\frac{\partial F}{\partial f_c} = \frac{(z_c - z_r)(f_c - f_r)}{\log\left(\frac{f_r}{f_c}\right)^2 f_c} + \frac{z_c - z_r}{\log\left(\frac{f_r}{f_c}\right)} - \frac{(z_c - z_l)(f_c - f_l)}{\log\left(\frac{f_l}{f_c}\right)^2 f_c} + \frac{z_l - z_c}{\log\left(\frac{f_l}{f_c}\right)} \tag{105}$$

This Newton's method iteration can be simplified, for $\psi = \frac{F}{f_c \frac{\partial F}{\partial f_c}}$, to

$$f_c^* = f_c\,\frac{(1 - \min(\psi, 0))}{(1 + \max(\psi, 0))} \tag{106}$$

Once the Newton's iteration has converged to an f_c, the interpolating function is given by (100) with $z = z_c$. An example of this interpolating function is shown in Figure 4. This interpolation is not neccesarily very smooth, but it is continous and captures the power-law nature of the underlying function.

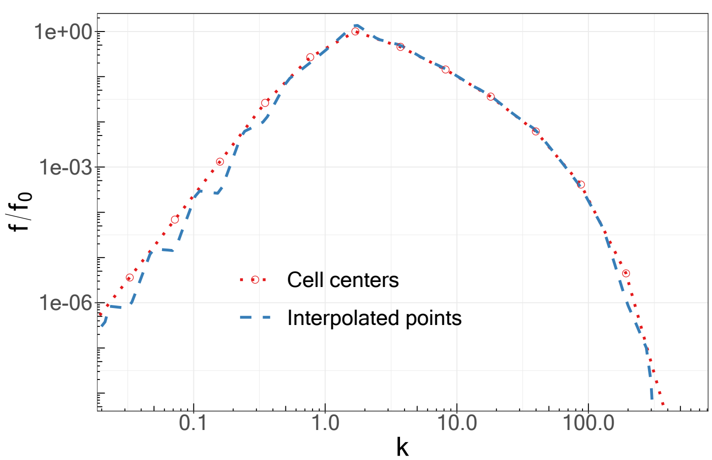

Figure 4 – Example of the interpolating function used in REA. The red dotted line is the original coarse-grid function, and the blue dashed line is the fine grid interpolation.

4. Model Evaluation

The LWN model in xRage is in a preliminary state, but several basic test problems are tested to evaluate the qualitative ability of the model to capture various canonical problems of interest.

4.1. Decaying Isotropic Turbulence

The decay of a field of homogenous isotropic turbulence is considered. The initial velocity field contains a spectrum of the form $E(k) = Ak^4 \exp\left(-2\frac{k^2}{k_0^2}\right)$, and time is normalized by the initial eddy turnover time $\tau_0 = L_I\sqrt{\frac{3}{R_{nn}(t=0)}}$. The turbulence is described by a Taylor Reynolds number,

$$Re_\lambda = \frac{u_{rms}\lambda}{\nu} \tag{107}$$

Where $u_{rms} = \sqrt{R_{nn}/3}$. The Taylor microscale is approximated by its value in isotropic uniform density turbulence,

$$\lambda \approx \sqrt{\frac{10\nu K}{\varepsilon}} \tag{108}$$

Where ε is the dissiption of turbulent kinetic energy per unit mass, $\varepsilon = \nu\int_0^\infty k^2 R_{nn}(k)dk$. First, we consider a high Reynolds number case with an initial $Re_\lambda = 5E6$, for which the compensated energy spectrum is plotted at different times in Figure 5. The wavenumbers are normalized by the Kolmogorov lengthscale, which is defined as $\eta = \left(\frac{\nu^3}{\varepsilon}\right)^{\frac{1}{4}}$. The energy spectrum of the turbulence relaxes to a $k^{\frac{5}{3}}$ slope and reproduces the $C_k = 1.8$ coefficient on the spectrum as prescribed by the cascade coefficients C'_{r1} and C'_{r2}. The normalized dissipation rate $D = \varepsilon L_I/u_{rms}^3$ in LWN asymptotes to roughly $D = 0.6$, whereas high Reynolds number DNS observes values closer to $D = 0.4 - 0.5$ [24]. Running at lower Reynolds number, $Re_\lambda = 72$, as shown in Figure 6, LWN likewise overpredicts the dissipation rate relative to the DNS of Samtaney et al [25]. The DNS includes turbulent Mach number effects, but at $M_t = 0.1$ these are unlikely to explain the difference. The difference may arise from this being a transitional flow at relatively low Reynolds number or from differences in the energy held at low wavenumbers, due to the difficulty in modeling backscatter in a robust manner.

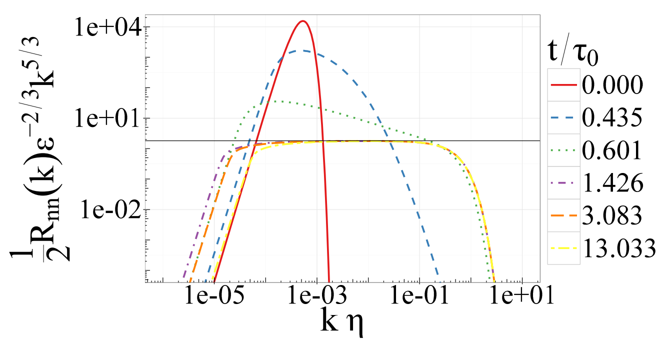

Figure 5 – Compensated spectrum of turbulent kinetic energy in decaying isotropic turbulence, with a large initial Reynolds number. The lines show spectra at different times throughout the simulation, and the black horizontal line is a reference line plotted at $y = 1.8$

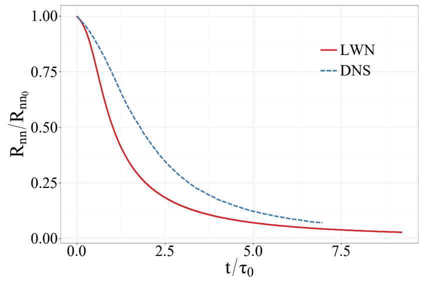

Figure 6 – Decay of isotropic turbulence, with an initial Reynolds number of $Re_\lambda = 72$. The DNS is from Samtaney et al. [25].

4.2. Homogenous Variable-Density Turbulence

Homogenous Variable Density Turbulent (HVDT) investigates a statistically homogenous field of density fluctuations which is driven to turbulence by gravity-driven buoyancy forces. Here we compare to the $A_t = 0.05$ and $A_t = 0.75$ DNS performed by [26] and also considered as a test problem for LWN in [10]. LWN is initialized from $t = 0$ by matching the initial value of b, and assuming a top-hat spectrum between wavenumbers 3 and 5. The DNS is initialized with a similar tophat spectrum but sharpens the interfaces between the materials and then applies a specific initial diffusion scale. Wavenumber space is discretized into $N_k = 128$ modes between $z_{lo} = -4$ and $z_{hi} = 10$, where $z = z_o \log k/k_0$. Time is normalized as $\tau = t/\sqrt{A_t g/L_0}$, where L_0 is an integral lengthscale of the initial density fluctuations,

$$L_0 = 2\pi \frac{\int_0^\infty b(k)k^{-1}dk}{\int_0^\infty b(k)dk} \tag{109}$$

The DNS is normalized by the lengthscale associate with the spectrum of ρ' instead of $b(k)$, but at low Atwood numbers these are similar metrics. The LWN reference lengthscale is $L_0 \approx 1.7$ and is larger than the lengthscales of the DNS $L_0 = 1.3 - 1.4$ [26], likely due to differences in the initial field. The viscosity is set by the Reynolds number $Re_0 = 10000$ ($A_t = 0.05$) and $Re_0 = 1563$ ($A_t = 0.75$), as $\nu = \sqrt{A_t g}L_0^{3/2}/Re_0$.

The behavior of several integral statistics from LWN is shown in Figure 7 through Figure 10. Generally, LWN does a reasonable job reproducing the DNS, although transition of K and b appears to occur too quickly. The degree of agreement between LWN and DNS is arguably worse than level of agreement seen in [1], but we note that here LWN is initialized from $t = 0$ and using coefficients tuned for other problems. Figure 8 shows spectra of several statistics relative to the DNS at different times.

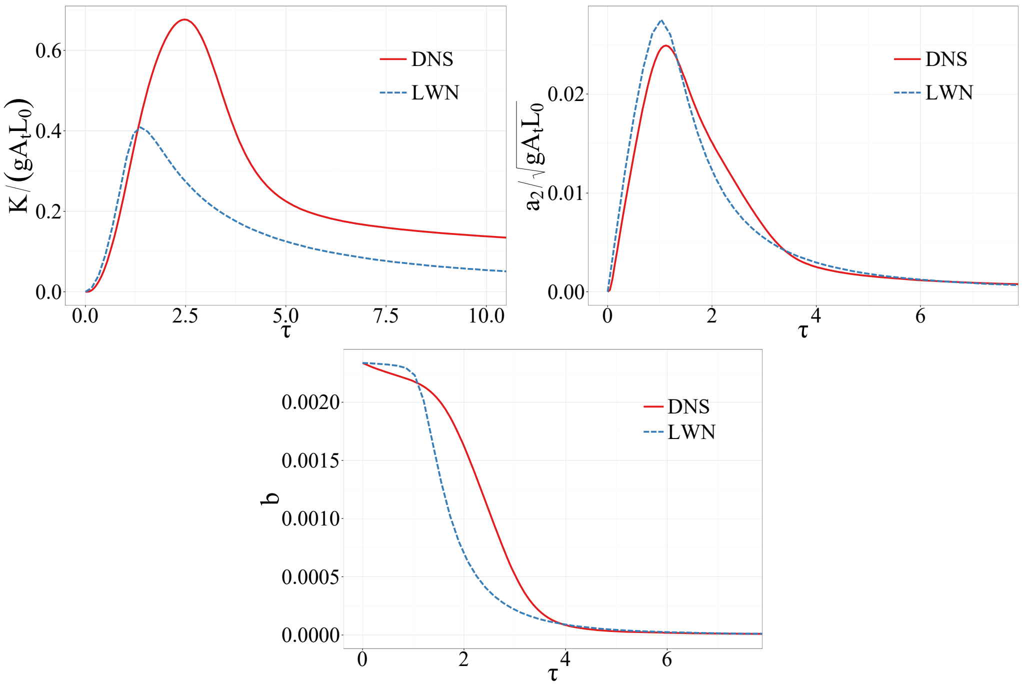

Figure 7 – Mean statistics in homogenous buoyancy driven turbulence at $A_t = 0.05$. *The DNS is from Aslangil et al. [26].*

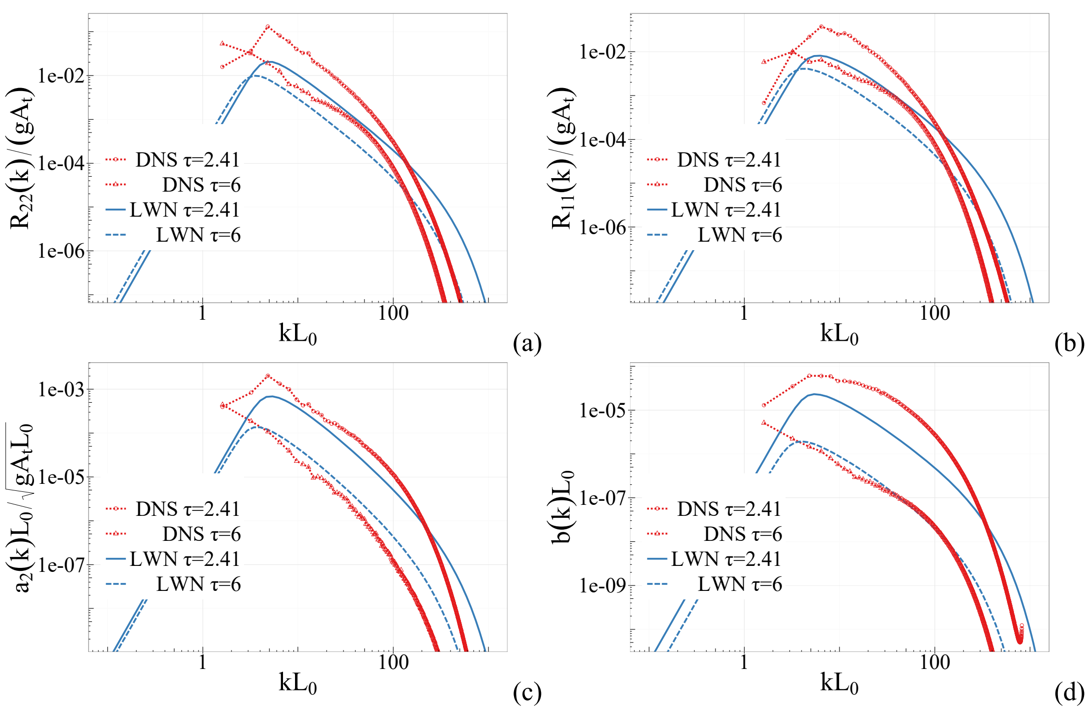

Figure 8 – Spectra of turbulent statistics in homogenous buoyancy driven turbulence with $A_t = 0.05$. *The DNS is from Aslangil et al. [26].*

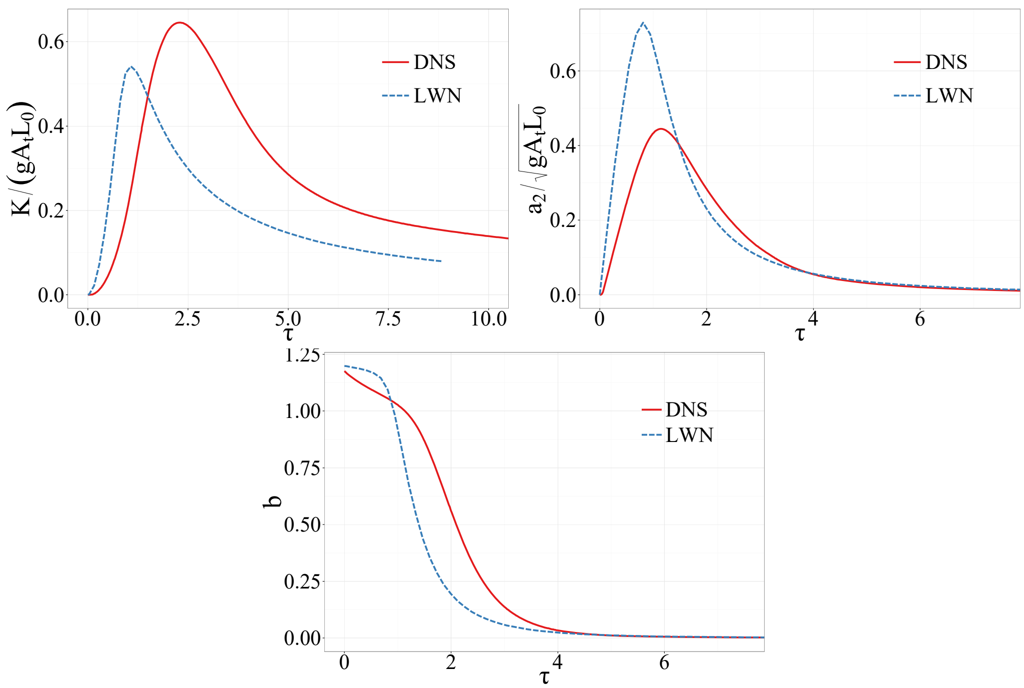

Figure 9 – Mean statistics in homogenous buoyancy driven turbulence at $A_t = 0.75$. The DNS is from Aslangil et al. [26].

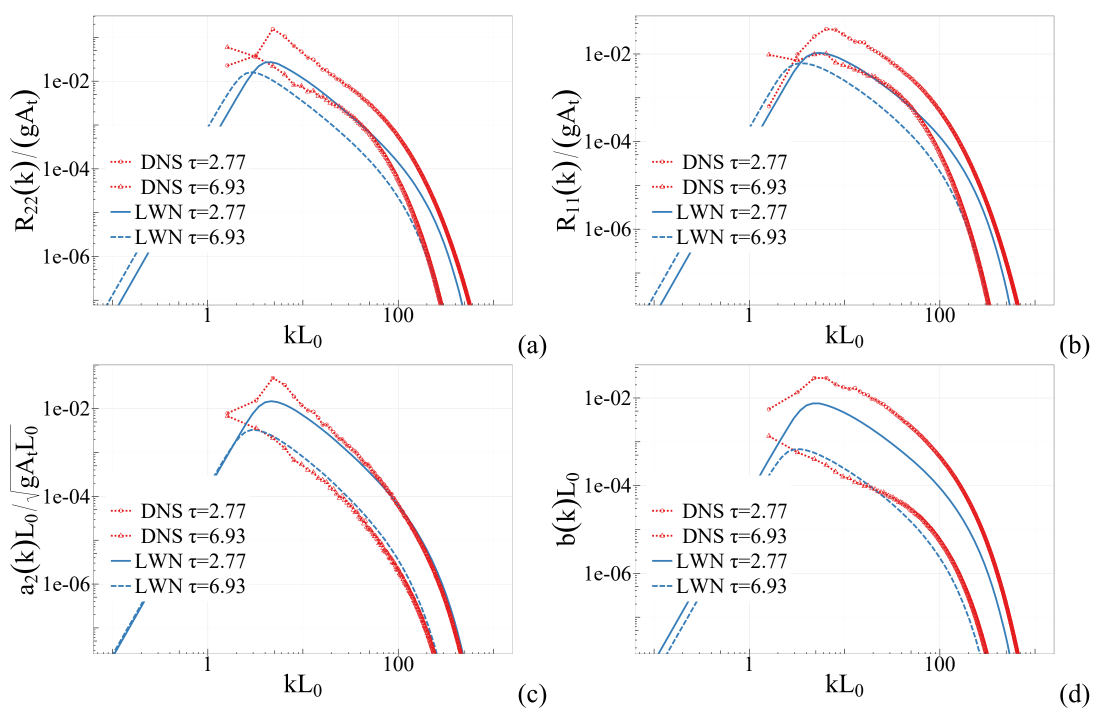

Figure 10 – Spectra of turbulent statistics in homogenous buoyancy driven turbulence with $A_t = 0.75$. The DNS is from Aslangil et al. [26].

4.3. Shock-Driven Turbulence

LWN is compared to the Richtmyer-Meshkov (RM) simulations of Wong et al. [21], which considers a $M_s = 1.45$ shock impacting an $A_t = 0.68$ interface between air and SF6, with reshock. The mixing layer width is defined

$$W = 4\int_0^\infty \bar{c}_{SF_6}\left(1 - \bar{c}_{SF_6}\right)dx \tag{110}$$

Although $\tilde{c}_{SF_6}$ is used in place of $\bar{c}_{SF_6}$ when calculating W in LWN. These can be translated using $\tilde{c}^k = \bar{c}^k - b^k$, but doing so lead to spurious discontinuities in the mixed width when b was rapidly chaning at a shock. The TKE is integrated in the transverse directions of the $30.0 \times 2.5 \times 2.5\ cm^3$ domain of the DNS. LWN is initialized with a top-hat spectrum in b over wavenumbers 50-60 cm^{-1}. The DNS initial conditions contain a broad diffusion layer, and the initial integrated value of b is set to 0.00321 times its configurational value to match the diffuse condition. Figure 11 compares the mixing layer width and integrated turbulent kinetic energy to the DNS, with which it sees reasonable agreement.

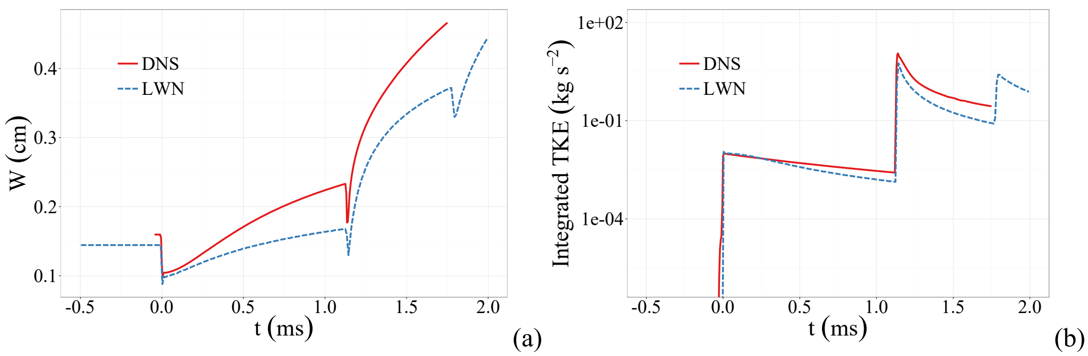

Figure 11 – Mixing layer width (a) and TKE integrated over the transverse directions (b) in a $M_s = 1.45$, $A_t = 0.68$ RM simulation. The DNS is from Wong et al [21].

4.4. Rayleigh-Taylor Turbulence

We compare to the Rayleigh-Taylor simulations of Livescu et al. [18]. All considered simulations have $Re_0 = 500$ and $L_0 = \frac{2\pi}{32}$, with viscosity again set by $\nu = \sqrt{A_t g L_0^{3/2}}\,/Re_0$. These cases are run with $N_k = 40$ wavenumber bins between $z_{lo} = -4$ and $z_{hi} = 11$,and a tophat initial condition on $b(k)$ over wavenumbers 30 to 34.

Figure 12 shows several integral statistics from an $A_t = 0.5$ case with gravity reversed at $\tau = 16$, while Figure 13 is an $A_t = 0.9$ case with a constant gravity field. LWN strongly overpredicts b during the transitional phase of the flow and appears to reach self-similarity quicker than the DNS. Most features of the DNS results are reproduced in LWN, and LWN is capable of capturing the 'de-mixing' behavior, where the mixing layer shrinks after gravity is reversed in the $A_t = 0.5$ case.

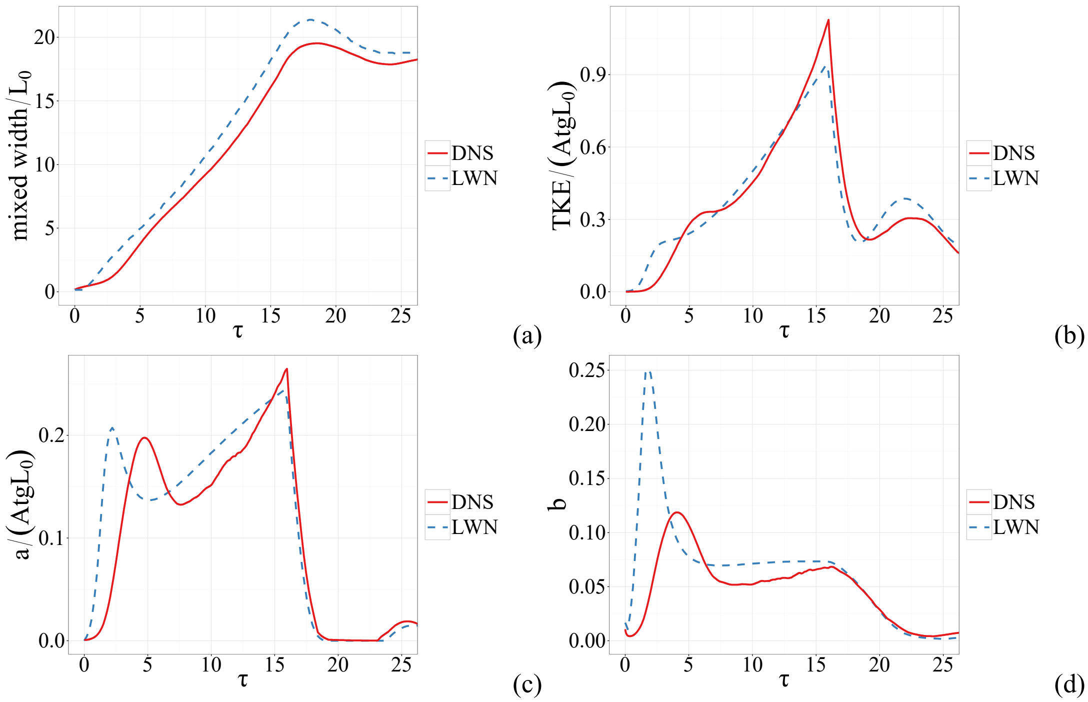

Figure 12 – Mixing layer width (a)and maximum values of turbulent kinetic energy (b), turbulent mass flux (c) and density-specific volume covariance (d), for an $A_t = 0.5$ Rayleigh-Taylor instabilityu. The DNS is from Livescu et al. [18].

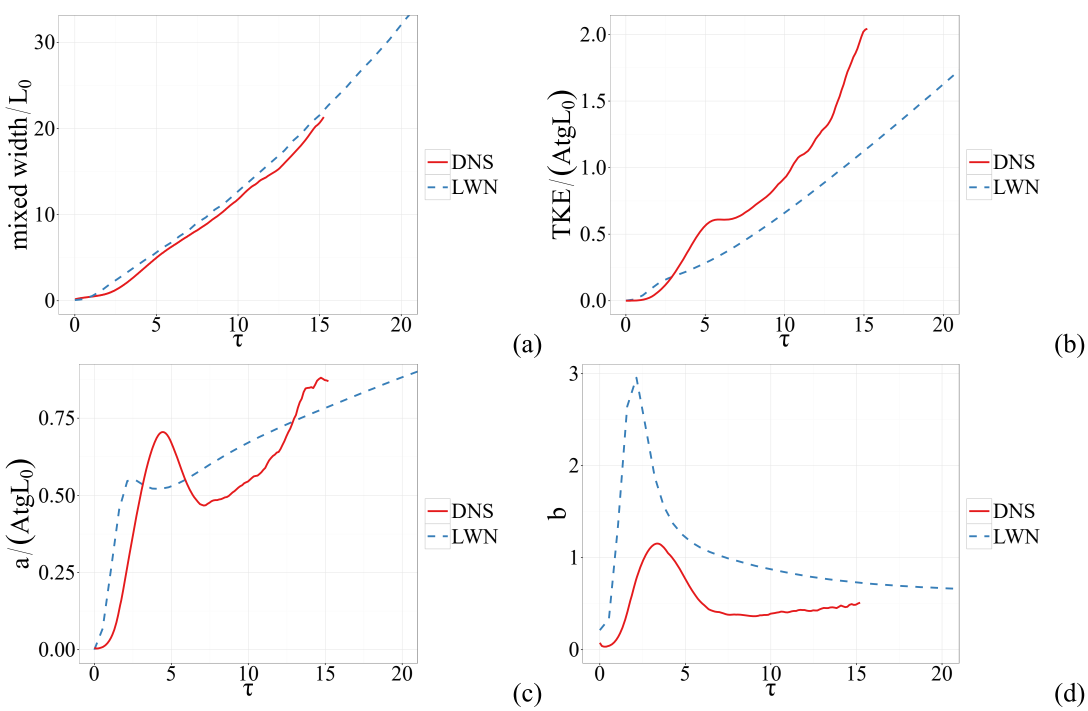

Figure 13 – Mixing layer width (a)and maximum values of turbulent kinetic energy (b), turbulent mass flux (c) and density-specific volume covariance (d), for an $A_t = 0.9$ Rayleigh-Taylor instabilityu. The DNS is from Livescu et al. [18].

5. Summary

Updates one the LWN implementation in xRage [11] are presented, included backscatter modeling, mean flow compression modeling, and incorporation of the material transport models from BHR4. Spectral-space numerical interpolation schemes are used to reduce the computational cost of the model. Results from a variety of inhomogeneous, variable density turbulent flows including Rayleigh-Taylor and Richtmyer-Meshkov turbulence are presented, and LWN successfully captures the qualitative evolution of these flows. Further work on the model is needed to improve coefficient tuning, including comparing the fit of specific closure models against the corresponding exact terms calculated from DNS or experiment.

References

[1] N. Pal, I. Boureima, N. Braun, S. Kurien, P. Ramaprabhu and A. Lawrie, "Local Wave Number Model for Inhomogeneous Two-Fluid Mixing," *Physical Review E,* vol. 104, no. 2, p. 025105, 2021.

[2] N. Braun and R. Gore, "A multispecies turbulence model for the mixing and de-mixing of miscible fluids," *LA-UR-21-25311.*

[3] J. D. Schwarzkopf, D. Livescu, J. R. Baltzer, R. A. Gore and J. R. Ristorcelli, "A two-length scale turbulence model for single-phase multi-fluid mixing.," *Flow, Turbulence and Combustion,* vol. 96, no. 1, pp. 1-43, 2016.

[4] J. D. Schwarzkopf, D. Livescu, R. A. Gore, R. M. Rauenzahn and J. R. Ristorcelli, "Application of a second-moment closure model to mixing processes involving multicomponent miscible fluids," *Journal of Turbulence,* vol. 12, p. N49, 2011.

[5] D. Besnard, F. Harlow, R. Rauenzahn and C. Zemach, "Turbulence transport equations for variable-density turbulence and their relationship to two-field models," Technical Report LA-12303-MS. Los Alamos National Lab., NM (United States), 1992.

[6] K. Stalsberg-Zarling and R. Gore, "The BHR2 Turbulence Model: Incompressible Isotropic Decay, Rayleigh-Taylor, Kelvin-Helmholtz and Homogeneous Variable-Density Turbulence (U)," Los Alamos National Laboratory Technical Report(LA-UR-11-04773), 2011.

[7] J. Canfield, N. Denissen, M. Francois, R. Gore, R. Rauenzahn, J. Reisner and S. Shkoller, "A Comparison of Interface Growth Models Applied to Rayleigh--Taylor and Richtmyer--Meshkov Instabilities," *Journal of Fluids Engineering,* vol. 142, no. 12, p. 121108, 2020.

[8] N. O. Braun and R. A. Gore, "A passive model for the evolution of subgrid-scale instabilities in turbulent flow regimes," *Physica D: Nonlinear Phenomena,* vol. 404, p. 132373, 2020.

[9] B. Rollin and M. J. Andrews, "n generating initial conditions for turbulence models: the case of Rayleigh–Taylor instability turbulent mixing," *Journal of Turbulence,* vol. 14, no. 3, pp. 77-106, 2013.

[10] N. Pal, S. Kurien, T. Clark, D. Aslangil and D. Livescu, "Two-point spectral model for variable-density homogeneous turbulence," *Physical Review Fluids,* vol. 3, no. 12, p. 124608, 2018.

[11] S. Kurien, J. Canfield, N. Pal, R. Rauenzahn and J. A. Saenz, "Local Wavenumber Turbulence Model Implementation in xRAGE: L3 Milestone Report," *Los Alamos Technical Report,* Vols. LA-UR-19-29439, 2019.

[12] S. Kurien and N. Pal, "The local wavenumber model for computation of turbulent mixing," *Phil. Trans. R. Soc. A.,* vol. 380, p. 20210076, 2022.

[13] M. Steinkamp, T. Clark and F. Harlow, "Two-point description of two-fluid turbulent mixing—I. Model formulation," *International journal of multiphase flow,* vol. 25, no. 4, pp. 599-637, 1999.

[14] D. Besnard, F. Harlow, R. Rauenzahn and C. Zemach, "Spectral transport model for turbulence," *Theoretical and computational fluid dynamics,* vol. 8, no. 1, pp. 1-35, 1996.

[15] T. Clark and P. Spitz, "Two-point correlation equations for variable density turbulence," *Los Alamos National Lab. Tech Report LA-12671-MS,* 1995.

[16] T. T. Clark and C. Zemach, "A spectral model applied to homogeneous turbulence," *Physics of Fluids,* vol. 7, no. 7, pp. 1674-1694, 1995.

[17] M. Lesieur, P. Comte, Y. Dubief, E. Lamballais, O. Metais and S. Ossia, "From Two-Point Closures of Isotropic Turbulence to LES of Shear Flows," *Flow, turbulence and combustion,* vol. 6, no. 1-4, pp. 247-267, 2000.

[18] D. Livescu, T. Wei and P. Brady, "Rayleigh-Taylor instability with gravity reversal," *Physica D: Nonlinear Phenomena,* vol. 417, p. 132832, 2021.

[19] G. N. Coleman and N. N. Mansour, "Modeling the rapid spherical compression of isotropic turbulence," *Physics of Fluids A: Fluid Dynamics,* vol. 3, no. 9, pp. 2255-2259, 1991.

[20] L. Jacquin, C. Cambon and E. Blin, "Turbulence amplification by a shock wave and rapid distortion theory," *Physics of Fluids A: Fluid Dynamics,* vol. 5, no. 10, pp. 2539-2550, 1993.

[21] M. L. Wong, D. Livescu and S. K. Lele, "High-resolution Navier-Stokes simulations of Richtmyer-Meshkov instability with reshock," *Phys. Rev. Fluids,* vol. 4, no. 10, p. 104609, 2019.

[22] R. Schiestel, "Multiple-time-scale modeling of turbulent flows in one-point closures," *The Physics of Fluids,* vol. 30, pp. 722-731, 1987.

[23] S. Pope, "Turbulent Flows," *Cambridge University Press,* p. 141, 2000.

[24] T. Ishihara, K. Morishita, M. Yokokawa, A. Uno and Y. Kaneda, "Energy spectrum in high-resolution direct numerical simulations of turbulence," *Phys. Rev. Fluids,* vol. 1, no. 9, p. 082403, 2016.

[25] R. Samtaney, D. I. Pullin and B. Kosovic, "Direct numerical simulation of decaying compressible turbulence and shocklet statistics," *Physics of Fluids,* vol. 13, no. 5, pp. 1415-1430, 2001.

[26] D. Aslangil, D. Livescu and A. Banerjee, "Effects of Atwood and Reynolds numbers on the evolution of buoyancy-driven homogeneous variable-density turbulence," *Journal of Fluid Mechanics,* vol. 895, 2020.

A. Appendix – Two-Point Transport Equation Derivations

Derivations for the two-point equations used here are provided below. These have not been been thoroughly checked and can almost certainly be further simplified, but this appendix is included in the hope that these could be useful as a starting position for further analysis.

To reduce clutter, the $\frac{r}{2}$ terms are dropped, e.g. $f(x+\frac{r}{2})$ is written $f(x+r)$. The math is the same and this allows the equations to be written in a shorter form.

The equations have colored terms. The colors should be considered arbitrary, but each term retains its original color (to the degree that this is possible). The colors are intended to help in tracking terms as they split and move around the equations, and to make it easier to do term-by-term comparisons between single-point and two-point forms.

A.1. R_{ij} Equation

Define:

$$R_{ij}(x,r) = \frac{\overline{\rho(x+r)u_i''(x-r)u_n''(x+r)}}{\bar{\rho}(x+r)}$$

$$a_n(x,r) = \frac{\overline{\rho'(x+r)u_n''(x-r)}}{\bar{\rho}(x-r)}$$

$$\sigma_{ij} = -P\delta_{ij} + \tau_{ij}$$

Start with the equations from Clark and Spitz [15]

$$\frac{\partial u_i''}{\partial t} + u_n''(\tilde{u}_i + u_i'')_{,n} + \tilde{u}_n u_{i,n}'' = \left(\bar{v} - \frac{1}{\bar{\rho}}\right)\bar{\sigma}_{ni,n} + v'\bar{\sigma}_{ni,n} + v\sigma_{ni,n}' + \frac{1}{\bar{\rho}}(\bar{\rho}R_{ni})_{,n} \tag{111}$$

$$\frac{\partial \rho u_i''}{\partial t} + \left(\rho u_i''(\tilde{u}_n + u_n'')\right)_{,n} + \rho u_n''\tilde{u}_{i,n} = \sigma_{ni,n}' - \frac{\rho'}{\bar{\rho}}\bar{\sigma}_{ni,n} + \left(1 + \frac{\rho'}{\bar{\rho}}\right)(\bar{\rho}R_{ni})_{,n} \tag{112}$$

Multiply (111) evaluated at x-r by (112) evaluated at x+r,

$$\frac{\partial \rho(x+r)u_i''(x-r)u_j''(x+r)}{\partial t} = u_i''(x-r)\frac{\partial \rho(x+r)u_j''(x+r)}{\partial t} + \rho(x+r)u_j''(x+r)\frac{\partial u_i''(x-r)}{\partial t} = \cdots \tag{113}$$

We can write the RHS side in either one-point form (where $r = 0$) or retain the two-point form,

One-Point (BHR)	$\begin{aligned} &= -u_j''(\rho u_i''\tilde{u}_n)_{,n} - u_j''(\rho u_i''u_n'')_{,n} - \rho u_n''u_j''\tilde{u}_{i,n} + u_j''\sigma'_{ni,n} - \frac{\rho' u_j''}{\bar{\rho}}\bar{\sigma}_{ni,n} + u_j''R_{ni,n} + \frac{\rho' u_j''}{\bar{\rho}}R_{ni,n} \\ &\quad - \rho u_i''u_n''\tilde{u}_{j,n} - \rho u_i''u_n''u_{j,n}'' - \tilde{u}_n\rho u_i''u_{j,n}'' + \rho u_i''\left(\bar{\nu} - \frac{1}{\bar{\rho}}\right)\bar{\sigma}_{nj,n} + \rho u_i''\nu'\bar{\sigma}_{nj,n} \\ &\quad + \rho u_i''\nu\sigma'_{nj,n} + \frac{\rho u_i''}{\bar{\rho}}(\bar{\rho}R_{nj})_{,n} \end{aligned}$	(114)
Two-Point (LWN)	$\begin{aligned} &= -u_i''(x-r)\Big(\rho(x+r)u_j''(x+r)\tilde{u}_n(x+r)\Big)_{,n} - u_i''(x-r)\Big(\rho(x+r)u_j''(x+r)u_n''(x+r)\Big)_{,n} \\ &\quad - \rho(x+r)u_i''(x-r)u_n''(x+r)\tilde{u}_{j,n}(x+r) + u_i''(x-r)\sigma'_{nj,n}(x+r) \\ &\quad - u_i''(x-r)\frac{\rho'(x+r)}{\bar{\rho}(x+r)}\bar{\sigma}_{nj,n}(x+r) + u_i''(x-r)\Big(\bar{\rho}(x+r)R_{nj}(x+r,0)\Big)_{,n} \\ &\quad + u_i''(x-r)\frac{\rho'(x+r)}{\bar{\rho}(x+r)}\Big(\bar{\rho}(x+r)R_{nj}(x+r,0)\Big)_{,n} \\ &\quad - \rho(x+r)u_j''(x+r)u_n''(x-r)\tilde{u}_{i,n}(x-r) \\ &\quad - \rho(x+r)u_j''(x+r)u_n''(x-r)u_{i,n}''(x-r) \\ &\quad - \rho(x+r)u_j''(x+r)\tilde{u}_n(x-r)u_{i,n}''(x-r) \\ &\quad + \rho(x+r)u_j''(x+r)\left(\bar{\nu}(x-r) - \frac{1}{\bar{\rho}(x-r)}\right)\bar{\sigma}_{ni,n}(x-r) \\ &\quad + \rho(x+r)u_j''(x+r)\nu'(x-r)\bar{\sigma}_{ni,n}(x-r) \\ &\quad + \rho(x+r)u_j''(x+r)\nu(x-r)\sigma'_{ni,n}(x-r) \\ &\quad + \frac{\rho(x+r)u_j''(x+r)}{\bar{\rho}(x-r)}\Big(\bar{\rho}(x-r)R_{ni}(x-r)\Big)_{,n} \end{aligned}$	(115)

With some simplifications to work towards the BHR3.1 form,

One-Point (BHR)	$\begin{aligned} &= -\left(\rho u_i''u_j''\tilde{u}_n\right)_{,n} + \rho u_i''u_{j,n}''\tilde{u}_n - \rho u_i''u_{j,n}''\tilde{u}_n - \left(\rho u_i''u_j''u_n''\right)_{,n} + \rho u_i''u_n''u_{j,n}'' - \rho u_i''u_n''u_{j,n}'' \\ &\quad - \rho u_j''u_n''\tilde{u}_{i,n} - \rho u_i''u_n''\tilde{u}_{j,n} + u_j''\sigma'_{ni,n} + \rho u_i''\nu\sigma'_{nj,n} - \frac{\rho' u_j''}{\bar{\rho}}\bar{\sigma}_{ni,n} \\ &\quad + \rho u_i''\left(\bar{\nu} - \frac{1}{\bar{\rho}}\right)\bar{\sigma}_{nj,n} + \rho u_i''\nu'\bar{\sigma}_{nj,n} + \frac{\rho u_i''}{\bar{\rho}}(\bar{\rho}R_{nj})_{,n} + \frac{\rho' u_j''}{\bar{\rho}}R_{ni,n} + u_j''R_{ni,n} \end{aligned}$	(116)
Two-Point (LWN)	$\begin{aligned} &= -\Big(\rho(x+r)u_i''(x-r)u_j''(x+r)\tilde{u}_n(x+r)\Big)_{,n} + \rho(x+r)u_j''(x+r)\tilde{u}_n(x+r)u_{i,n}''(x-r) \\ &\quad - \rho(x+r)u_j''(x+r)\tilde{u}_n(x-r)u_{i,n}''(x-r) \\ &\quad - \Big(\rho(x+r)u_i''(x-r)u_j''(x+r)u_n''(x+r)\Big)_{,n} \\ &\quad + \rho(x+r)u_j''(x+r)u_n''(x+r)u_{i,n}''(x-r) \\ &\quad - \rho(x+r)u_n''(x-r)u_j''(x+r)u_{i,n}''(x-r) \\ &\quad - \rho(x+r)u_i''(x-r)u_n''(x+r)\tilde{u}_{j,n}(x+r) \\ &\quad - \rho(x+r)u_n''(x-r)u_j''(x+r)\tilde{u}_{i,n}(x-r) + u_i''(x-r)\sigma'_{nj,n}(x+r) \\ &\quad + \rho(x+r)u_j''(x+r)\nu(x-r)\sigma'_{ni,n}(x-r) - u_i''(x-r)\frac{\rho'(x+r)}{\bar{\rho}(x+r)}\bar{\sigma}_{nj,n}(x+r) \\ &\quad + \rho(x+r)u_j''(x+r)\left(\bar{\nu}(x-r) - \frac{1}{\bar{\rho}(x-r)}\right)\bar{\sigma}_{ni,n}(x-r) \\ &\quad + \rho(x+r)u_j''(x+r)\nu'(x-r)\bar{\sigma}_{ni,n}(x-r) \\ &\quad + \frac{\rho(x+r)u_j''(x+r)}{\bar{\rho}(x-r)}\Big(\bar{\rho}(x-r)R_{ni}(x-r)\Big)_{,n} \\ &\quad + u_i''(x-r)\frac{\rho'(x+r)}{\bar{\rho}(x+r)}\Big(\bar{\rho}(x+r)R_{nj}(x+r,0)\Big)_{,n} \\ &\quad + u_i''(x-r)\Big(\bar{\rho}(x+r)R_{nj}(x+r,0)\Big)_{,n} \end{aligned}$	(117)

One-Point (BHR)	$\begin{aligned} &= -\left(\rho u_i'' u_j'' \tilde{u}_n\right)_{,n} - \left(\rho u_i'' u_j'' u_n''\right)_{,n} - \rho u_j'' u_n'' \tilde{u}_{i,n} - \rho u_i'' u_n'' \tilde{u}_{j,n} + u_j'' \sigma'_{ni,n} + \rho v u_i'' \sigma'_{nj,n} - \frac{\rho' u_j''}{\bar{\rho}} \bar{\sigma}_{ni,n} \\ &\quad + \rho u_i'' \left(\bar{v} - \frac{1}{\bar{\rho}}\right) \bar{\sigma}_{nj,n} + \rho u_i'' v' \bar{\sigma}_{nj,n} + \frac{\rho u_i''}{\bar{\rho}} \left(\bar{\rho} R_{nj}\right)_{,n} + \frac{\rho' u_j''}{\bar{\rho}} R_{ni,n} + u_j'' R_{ni,n} \end{aligned}$	(118)
Two-Point (LWN)	$\begin{aligned} &= -\left(\rho(x+r) u_i''(x-r) u_j''(x+r) \tilde{u}_n(x+r)\right)_{,n} - \left(\rho(x+r) u_i''(x-r) u_j''(x+r) u_n''(x+r)\right)_{,n} \\ &\quad - \rho(x+r) u_i''(x-r) u_n''(x+r) \tilde{u}_{j,n}(x+r) \\ &\quad - \rho(x+r) u_n''(x-r) u_j''(x+r) \tilde{u}_{i,n}(x-r) + u_i''(x-r) \sigma'_{nj,n}(x+r) \\ &\quad + \rho(x+r) u_j''(x+r) v(x-r) \sigma'_{ni,n}(x-r) - u_i''(x-r) \frac{\rho'(x+r)}{\bar{\rho}(x+r)} \bar{\sigma}_{nj,n}(x+r) \\ &\quad + \rho(x+r) u_j''(x+r) \left(\bar{v}(x-r) - \frac{1}{\bar{\rho}(x-r)}\right) \bar{\sigma}_{ni,n}(x-r) \\ &\quad + \rho(x+r) u_j''(x+r) v'(x-r) \bar{\sigma}_{ni,n}(x-r) \\ &\quad + \frac{\rho(x+r) u_j''(x+r)}{\bar{\rho}(x-r)} \left(\bar{\rho}(x-r) R_{ni}(x-r)\right)_{,n} \\ &\quad + \frac{\rho'(x+r) u_i''(x-r)}{\bar{\rho}(x+r)} \left(\bar{\rho}(x+r) R_{nj}(x+r,0)\right)_{,n} \\ &\quad + u_i''(x-r) \left(\bar{\rho}(x+r) R_{nj}(x+r,0)\right)_{,n} \\ &\quad + \left\{\rho(x+r) u_j''(x+r) u_{i,n}''(x-r) \left(\tilde{u}_n(x+r) - \tilde{u}_n(x-r)\right)\right\} \\ &\quad + \left\{\rho(x+r) u_j''(x+r) u_n''(x+r) u_{i,n}''(x-r) \right. \\ &\quad \left. - \rho(x+r) u_n''(x-r) u_j''(x+r) u_{i,n}''(x-r)\right\} \end{aligned}$	(119)

Average, $R_{ij} = \frac{\overline{\rho u_i'' u_j''}}{\bar{\rho}}$, use $\rho v u_i'' \sigma'_{nj,n} = u_i'' \sigma'_{nj,n}$ in the 1-point form

One-Point (BHR)	$\begin{aligned} &= -\left(\bar{\rho} R_{ij} \tilde{u}_n\right)_{,n} - \left(\overline{\rho u_i'' u_j'' u_n''}\right)_{,n} - \bar{\rho} R_{jn} \tilde{u}_{i,n} - \bar{\rho} R_{in} \tilde{u}_{j,n} + \overline{u_j'' \sigma'_{ni,n}} + \overline{u_i'' \sigma'_{nj,n}} - a_j \bar{\sigma}_{ni,n} + \overline{\rho u_i'' v'} \bar{\sigma}_{nj,n} \\ &\quad + a_j R_{ni,n} - a_j R_{ni,n} \end{aligned}$	(120)
Two-Point (LWN)	$\begin{aligned} &= -\left(\overline{\rho(x+r) u_i''(x-r) u_j''(x+r)} \tilde{u}_n(x+r)\right)_{,n} - \left(\overline{\rho(x+r) u_i''(x-r) u_j''(x+r) u_n''(x+r)}\right)_{,n} \\ &\quad - \overline{\rho(x+r) u_i''(x-r) u_n''(x+r)} \tilde{u}_{j,n}(x+r) \\ &\quad - \overline{\rho(x+r) u_n''(x-r) u_j''(x+r)} \tilde{u}_{i,n}(x-r) + \overline{u_i''(x-r) \sigma'_{nj,n}(x+r)} \\ &\quad + \overline{\rho(x+r) v(x-r) u_j''(x+r) \sigma'_{ni,n}(x-r)} - \frac{\overline{\rho'(x+r) u_i''(x-r)}}{\bar{\rho}(x+r)} \bar{\sigma}_{nj,n}(x+r) \\ &\quad + \overline{\rho(x+r) u_j''(x+r) v'(x-r)} \bar{\sigma}_{ni,n}(x-r) \\ &\quad + \frac{\overline{\rho'(x+r) u_i''(x-r)}}{\bar{\rho}(x+r)} \left(\bar{\rho}(x+r) R_{nj}(x+r,0)\right)_{,n} \\ &\quad + \overline{u_i''(x-r)} \left(\bar{\rho}(x+r) R_{nj}(x+r,0)\right)_{,n} \\ &\quad + \left\{\overline{\rho(x+r) u_j''(x+r) u_{i,n}''(x-r)} \left(\tilde{u}_n(x+r) - \tilde{u}_n(x-r)\right)\right\} \\ &\quad + \left\{\overline{\rho(x+r) u_j''(x+r) u_n''(x+r) u_{i,n}''(x-r)} \right. \\ &\quad \left. - \overline{\rho(x+r) u_n''(x-r) u_j''(x+r) u_{i,n}''(x-r)}\right\} \end{aligned}$	(121)

Note the following (this is only used in the 2-point form)

One-Point (BHR)	$\overline{u_j''\sigma_{ni,n}'} + \overline{u_i''\sigma_{nj,n}'} = \left(\overline{u_j''\sigma_{ni}'} + \overline{u_i''\sigma_{nj}'}\right)_{,n} - \overline{u_{j,n}''\sigma_{ni}'} - \overline{u_{i,n}''\sigma_{nj}'}$	(122)
Two-Point (LWN)	$\overline{u_i''(x-r)\sigma_{nj,n}'(x+r)} + \overline{\rho(x+r)v(x-r)u_j''(x+r)\sigma_{ni,n}'(x-r)}$ $= \left(\overline{u_i''(x-r)\sigma_{nj}'(x+r)} + \overline{\rho(x+r)v(x-r)u_j''(x+r)\sigma_{ni}'(x-r)}\right)_{,n}$ $- \overline{u_{i,n}''(x-r)\sigma_{nj}'(x+r)} - \overline{\left(\rho(x+r)v(x-r)u_j''(x+r)\right)_{,n}\sigma_{ni}'(x-r)}$	(123)

And

One-Point (BHR)	$\overline{\rho u_i''v'}\bar{\sigma}_{nj,n} = \bar{\rho}\,\overline{u_i''v'}\bar{\sigma}_{nj,n} + \overline{\rho'v'u_i''}\bar{\sigma}_{nj,n}$ $= (1-\bar{\rho}\bar{v})\overline{u_i''}\bar{\sigma}_{nj,n} - \bar{v}\,\overline{u_i''\rho'}\bar{\sigma}_{nj,n} - \overline{\rho'v'u_i''}\bar{\sigma}_{nj,n} + \overline{\rho'v'u_i''}\bar{\sigma}_{nj,n}$ $= (\bar{\rho}\bar{v}-1)a_i\bar{\sigma}_{nj,n} - \bar{\rho}\bar{v}a_i\,\bar{\sigma}_{nj,n}$ $\overline{\rho u_i''v'}\bar{\sigma}_{nj,n} = -a_i\bar{\sigma}_{nj,n}$	(124)
Two-Point (LWN)	$\overline{\rho(x+r)u_j''(x+r)v'(x-r)}\bar{\sigma}_{ni,n}(x-r)$ $= \left[\bar{\rho}(x+r)\bar{v}(x-r) - (b(x-r,0)+1)\frac{\bar{\rho}(x+r)}{\bar{\rho}(x-r)}\right]a_j(x+r,0)\bar{\sigma}_{ni,n}(x-r)$ $+ \left(\overline{\rho'(x+r)v'(x-r)u_j'(x+r)}\right.$ $\left.- \frac{\bar{\rho}(x+r)}{\bar{\rho}(x-r)}\overline{\rho'(x-r)v'(x-r)u_j'(x+r)}\right)\bar{\sigma}_{ni,n}(x-r)$ $- \left\{\bar{\rho}(x+r)\bar{v}(x-r)\frac{\bar{\rho}(x+r)}{\bar{\rho}(x-r)}a_j(x,-r) - b(x,r)a_j(x+r,0)\right\}\bar{\sigma}_{ni,n}(x-r)$	(125)

Going back to the full equation, at this point the 1-point form is now in the basic form used by BHR [4].

One-Point (BHR)	$\begin{aligned} = &-\left(\bar{\rho}R_{ij}\tilde{u}_n\right)_{,n} - \left(\overline{\rho u_i'' u_j'' u_n''}\right)_{,n} - \bar{\rho}R_{jn}\tilde{u}_{i,n} - \bar{\rho}R_{in}\tilde{u}_{j,n} + \overline{u_j''\sigma_{ni,n}'} + \overline{u_i''\sigma_{nj,n}'} - a_j\bar{\sigma}_{ni,n} \\ &- a_i\bar{\sigma}_{nj,n} \end{aligned}$	(126)
Two-Point (LWN)	$\begin{aligned} = &-\left(\bar{\rho}(x+r)R_{ij}(x,r)\tilde{u}_n(x+r)\right)_{,n} - \left(\overline{\rho(x+r)u_i''(x-r)u_j''(x+r)u_n''(x+r)}\right)_{,n} \\ &- \bar{\rho}(x+r)R_{in}(x,r)\tilde{u}_{j,n}(x+r) - \bar{\rho}(x+r)R_{nj}(x,r)\tilde{u}_{i,n}(x-r) \\ &+ \left(\overline{u_i''(x-r)\sigma_{nj}'(x+r)} + \overline{\rho(x+r)\nu(x-r)u_j''(x+r)\sigma_{ni}'(x-r)}\right)_{,n} \\ &- \overline{u_{i,n}''(x-r)\sigma_{nj}'(x+r)} - \overline{\left(\rho(x+r)\nu(x-r)u_j''(x+r)\right)_{,n}\sigma_{ni}'(x-r)} \\ &- \frac{\bar{\rho}(x-r)}{\bar{\rho}(x+r)}\,a(x,r)\bar{\sigma}_{nj,n}(x+r) \\ &- \left\{\bar{\rho}(x+r)\bar{\nu}(x-r)\frac{\bar{\rho}(x+r)}{\bar{\rho}(x-r)}a_j(x,-r) - b(x,r)a_j(x+r,0)\right\}\bar{\sigma}_{ni,n}(x \\ &- r) + \left\{\overline{\rho(x+r)u_j''(x+r)u_{i,n}''(x-r)}\left(\tilde{u}_n(x+r) - \tilde{u}_n(x-r)\right)\right\} \\ &+ \{\overline{\rho(x+r)u_j''(x+r)u_n''(x+r)u_{i,n}''(x-r)} \\ &- \overline{\rho(x+r)u_n''(x-r)u_j''(x+r)u_{i,n}''(x-r)}\} \\ &+ \left\{\frac{\bar{\rho}(x-r)}{\bar{\rho}(x+r)}\,a_i(x,r)\left(\bar{\rho}(x+r)R_{nj}(x+r,0)\right)_{,n}\right. \\ &\left.- a_i(x-r,0)\left(\bar{\rho}(x+r)R_{nj}(x+r,0)\right)_{,n}\right\} \\ &+ \left[\bar{\rho}(x+r)\bar{\nu}(x-r) - (b(x-r,0)+1)\frac{\bar{\rho}(x+r)}{\bar{\rho}(x-r)}\right]a_j(x+r,0)\bar{\sigma}_{ni,n}(x \\ &- r) \\ &+ \left(\overline{\rho'(x+r)\nu'(x-r)u_j'(x+r)}\right. \\ &\left.- \frac{\bar{\rho}(x+r)}{\bar{\rho}(x-r)}\overline{\rho'(x-r)\nu'(x-r)u_j'(x+r)}\right)\bar{\sigma}_{ni,n}(x-r) \end{aligned}$	(127)

With some final reductions, we yield a relatively manageable form of the two-point R_{ij} equation. Again that that $x \pm r$ terms should be $x \pm \frac{r}{2}$, and in practice one probably should use a symmtetric verion of R_{ij}, such as $R_{ij}^{sym}(x,r) = \frac{1}{2}\left(R_{ij}(x,r) + R_{ij}(x,-r)\right)$.

One-Point (BHR)	$\begin{aligned} &\frac{\partial \bar{\rho} R_{ij}}{\partial t} + \left(\bar{\rho} R_{ij} \tilde{u}_n\right)_{,n} \\ &\quad = -\left(\overline{\rho u_i'' u_j'' u_n''}\right)_{,n} - \bar{\rho} R_{jn} \tilde{u}_{i,n} - \bar{\rho} R_{in} \tilde{u}_{j,n} + \overline{u_j'' \sigma'_{ni,n}} + \overline{u_i'' \sigma'_{nj,n}} - a_j \bar{\sigma}_{ni,n} \\ &\quad - a_i \bar{\sigma}_{nj,n} \end{aligned}$	(128)
Two-Point (LWN)	$\begin{aligned} &\frac{\partial \bar{\rho}(x+r) R_{ij}(x,r)}{\partial t} + \left(\bar{\rho}(x+r) R_{ij}(x,r) \tilde{u}_n(x+r)\right)_{,n} \\ &\quad = -\left(\overline{\rho(x+r) u_i'(x-r) u_j''(x+r) u_n''(x+r)}\right)_{,n} \\ &\quad - \bar{\rho}(x+r) R_{in}(x,r) \tilde{u}_{j,n}(x+r) - \bar{\rho}(x+r) R_{nj}(x,r) \tilde{u}_{i,n}(x-r) \\ &\quad + \left(\overline{u_i''(x-r) \sigma'_{nj}(x+r)} + \overline{\rho(x+r) \nu(x-r) u_j''(x+r) \sigma'_{ni}(x-r)}\right)_{,n} \\ &\quad - \overline{\left(\rho(x+r) \nu(x-r) u_j''(x+r)\right)_{,n} \sigma'_{ni}(x-r)} - \overline{u_{i,n}''(x-r) \sigma'_{nj}(x+r)} \\ &\quad - \frac{\bar{\rho}(x-r)}{\bar{\rho}(x+r)} a_i(x,r) \bar{\sigma}_{nj,n}(x+r) \\ &\quad - \left\{\bar{\rho}(x+r) \bar{\nu}(x-r) \frac{\bar{\rho}(x+r)}{\bar{\rho}(x-r)} a_j(x,-r) - b(x,r) a_j(x+r,0)\right\} \bar{\sigma}_{ni,n}(x \\ &\quad - r) \\ &\quad + \left\{\frac{\bar{\rho}(x-r)}{\bar{\rho}(x+r)} a_i(x,r) \left(\bar{\rho}(x+r) R_{nj}(x+r,0)\right)_{,n} \right. \\ &\quad \left. + \bar{\rho}(x+r) R_{nj}(x,r) a_{i,n}(x-r,0)\right\} \\ &\quad + \left\{\overline{\rho(x+r) u_j''(x+r) u_{i,n}''(x-r)}\left(\tilde{u}_n(x+r) - \tilde{u}_n(x-r)\right)\right\} \\ &\quad + \left\{\overline{\rho(x+r) u_j''(x+r) u_{i,n}'(x-r)\{u_n''(x+r) - u_n''(x-r)\}}\right\} \\ &\quad + \left(\overline{\rho'(x+r) \nu'(x-r) u_j'(x+r)} \right. \\ &\quad \left. - \frac{\bar{\rho}(x+r)}{\bar{\rho}(x-r)} \overline{\rho'(x-r) \nu'(x-r) u_j'(x+r)}\right) \bar{\sigma}_{ni,n}(x-r) \end{aligned}$	(129)

The two point form is the same as the 1-pt BHR equation as $r \to 0$ except we've split the transport term $\left(\overline{\rho u_i'' u_j'' u_n''}\right)_{,n}$ into $\left(\overline{\rho u_i' u_j'' u_n''} - \overline{\rho u_j'' u_n''} a_i\right)_{,n}$, creating a new term in the equation. This is to ensure that each term individually $\to 0$ as $r \to \infty$. We also use Reynolds averaging on the viscous stress tensor whereas Schwarzkopf 2011 used Favre averaging on that term.

$\overline{\rho u_i'' u_j'' u_n''}$ doesn't $\to 0$ in a trival manner as $r \to \infty$ because correlations between values of nonzero mean don't go to zero even if the terms are uncorrelated, e.g. $\overline{u''(x+r) u''(x-r)} = a^2$ as $r \to \infty$

A.2. a_i Equation

To derive the a equations, starting from Clark and Spitz [15] ρ' and u_i'' equations

$$\frac{\partial \rho'}{\partial t} + (\rho' \tilde{u}_n + \rho u_n'')_{,n} = 0$$

$$\frac{\partial u_i''}{\partial t} + \tilde{u}_n u_{i,n}'' + u_n'' u_{i,n} - \frac{1}{\bar{\rho}}(\bar{\rho} R_{ni})_{,n} = -\frac{1}{\bar{\rho}}\bar{\sigma}_{ni,n} + \frac{1}{\rho}\bar{\sigma}_{ni,n}$$

$$\frac{\partial u_i''}{\partial t} + u_n''(\tilde{u}_i + u_i'')_{,n} + \tilde{u}_n u_{i,n}'' = \left(\bar{v} - \frac{1}{\bar{\rho}}\right)\bar{\sigma}_{ni,n} + v'\bar{\sigma}_{ni,n} + v\sigma_{ni,n}' + \frac{1}{\bar{\rho}}(\bar{\rho} R_{ni})_{,n}$$

Define $a_n(x,r) = \frac{\overline{\rho'(x+r)u_n''(x-r)}}{\bar{\rho}(x-r)}$

$$\frac{\partial \rho'(x+r)u_i''(x-r)}{\partial t} = u_i''(x-r)\frac{\partial \rho'(x+r)}{\partial t} + \rho'(x+r)\frac{\partial u_i''(x-r)}{\partial t} = \cdots$$

One-Point (BHR)	$= -(\rho' u_i'' \tilde{u}_n)_{,n} + \rho' u_{i,n}'' \tilde{u}_n - (\rho u_i'' u_n'')_{,n} + \rho u_n'' u_{i,n}'' - u_n'' \rho' \tilde{u}_{i,n} - u_n'' \rho' u_{i,n}'' - \tilde{u}_n \rho' u_{i,n}''$ $+ \rho'\left(\bar{v} - \frac{1}{\bar{\rho}}\right)\bar{\sigma}_{ni,n} + \rho' v' \bar{\sigma}_{ni,n} + \rho' v \sigma_{ni,n}' + \frac{\rho'}{\bar{\rho}}(\bar{\rho} R_{ni})_{,n}$	(130)
Two-Point (LWN)	$= -\left(\rho'(x+r)u_i''(x-r)\tilde{u}_n(x+r)\right)_{,n} + \rho'(x+r)u_{i,n}''(x-r)\tilde{u}_n(x+r)$ $- \left(\rho(x+r)u_i''(x-r)u_n''(x+r)\right)_{,n} + \rho(x+r)u_n''(x+r)u_{i,n}''(x-r)$ $- \rho'(x+r)u_n''(x-r)\tilde{u}_{i,n}(x-r) - \rho'(x+r)u_n''(x-r)u_{i,n}''(x-r)$ $- \rho'(x+r)\tilde{u}_n(x-r)u_{i,n}''(x-r)$ $+ \rho'(x+r)\left(\bar{v}(x-r) - \frac{1}{\bar{\rho}(x-r)}\right)\bar{\sigma}_{ni,n}(x-r)$ $+ \rho'(x+r)v'(x-r)\bar{\sigma}_{ni,n}(x-r) + \rho'(x+r)v(x-r)\sigma_{ni,n}'(x-r)$ $+ \frac{\rho'(x+r)}{\bar{\rho}(x-r)}\left(\bar{\rho}(x-r)R_{ni}(x-r)\right)_{,n}$	(131)

Apply averaging:

One-Point (BHR)	$= -(\bar{\rho} a_i \tilde{u}_n)_{,n} + \overline{\rho' u_{i,n}''}\tilde{u}_n - (\overline{\rho u_i'' u_n''})_{,n} + \overline{\rho u_n'' u_{i,n}''} - \bar{\rho} a_n \tilde{u}_{i,n} - \overline{(u_n'' \rho' u_{i,n}'')} - \tilde{u}_n \overline{\rho' u_{i,n}''}$ $- b\bar{\sigma}_{ni,n} + \overline{\rho' v \sigma_{ni,n}'}$	(132)
Two-Point (LWN)	$= -\left(\overline{\rho'(x+r)u_i''(x-r)}\tilde{u}_n(x+r)\right)_{,n} + \overline{\rho'(x+r)u_{i,n}''(x-r)}\tilde{u}_n(x+r)$ $- \left(\overline{\rho(x+r)u_i''(x-r)u_n''(x+r)}\right)_{,n} + \overline{\rho(x+r)u_n''(x+r)u_{i,n}''(x-r)}$ $- \overline{\rho'(x+r)u_n''(x-r)}\tilde{u}_{i,n}(x-r) - \overline{\rho'(x+r)u_n''(x-r)u_{i,n}''(x-r)}$ $- \overline{\rho'(x+r)u_{i,n}''(x-r)}\tilde{u}_n(x-r) + \overline{\rho'(x+r)v'(x-r)}\bar{\sigma}_{ni,n}(x-r)$ $+ \overline{\rho'(x+r)v(x-r)\sigma_{ni,n}'(x-r)}$	(133)

Do some simplifying:

One-Point (BHR)	$\begin{aligned} &= -(\bar{\rho} a_i \tilde{u}_n)_{,n} + \overline{\rho' u''_{i,n}}\tilde{u}_n - (\bar{\rho} R_{in})_{,n} + \overline{\rho u''_n u''_{i,n}} - \bar{\rho} a_n \tilde{u}_{i,n} - \overline{(\rho' u''_n u''_{i,n})} - \tilde{u}_n \overline{\rho' u''_{i,n}} \\ &\quad - b\bar{\sigma}_{ni,n} + \bar{\nu}\overline{\rho' \sigma'_{ni,n}} + \overline{\nu' \rho' \sigma'_{ni,n}} \end{aligned}$	(134)
Two-Point (LWN)	$\begin{aligned} = &-\left(\overline{\rho'(x+r) u''_i(x-r)}\tilde{u}_n(x+r)\right)_{,n} + \overline{\rho'(x+r) u''_{i,n}(x-r)}\tilde{u}_n(x+r) \\ &- \left(\overline{\rho(x+r) u''_i(x-r) u''_n(x+r)}\right)_{,n} + \overline{\rho(x+r) u''_n(x+r) u''_{i,n}(x-r)} \\ &- \overline{\rho'(x+r) u''_n(x-r)}\tilde{u}_{i,n}(x-r) - \overline{\rho'(x+r) u''_n(x-r) u''_{i,n}(x-r)} \\ &- \overline{\rho'(x+r) u''_{i,n}(x-r)}\tilde{u}_n(x-r) + \overline{\rho'(x+r)\nu'(x-r)}\bar{\sigma}_{ni,n}(x-r) \\ &+ \bar{\nu}(x-r)\overline{\rho'(x+r)\sigma'_{ni,n}(x-r)} + \overline{\rho'(x+r)\nu'(x-r)\sigma'_{ni,n}(x-r)} \end{aligned}$	(135)

Using:

$$\begin{aligned} &\bar{\nu}(x-r)\overline{\rho'(x+r)\sigma'_{ni,n}(x-r)} \\ &\qquad = \frac{\bar{\nu}(x-r)}{\bar{\nu}(x+r)}\overline{\sigma'_{ni,n}(x-r)} - \bar{\nu}(x-r)\bar{\rho}(x+r)\overline{\sigma'_{ni,n}(x-r)} \\ &\qquad\quad - \frac{\bar{\nu}(x-r)\bar{\rho}(x+r)}{\bar{\nu}(x+r)}\overline{\nu'(x+r)\sigma'_{ni,n}(x-r)} - \frac{\bar{\nu}(x-r)}{\bar{\nu}(x+r)}\overline{\nu'(x+r)\rho'(x+r)\sigma'_{ni,n}(x-r)} \\ &\qquad = -\frac{\bar{\nu}(x-r)\bar{\rho}(x+r)}{\bar{\nu}(x+r)}\overline{\nu'(x+r)\sigma'_{ni,n}(x-r)} - \frac{\bar{\nu}(x-r)}{\bar{\nu}(x+r)}\overline{\nu'(x+r)\rho'(x+r)\sigma'_{ni,n}(x-r)} \end{aligned}$$

One-Point (BHR)	$\begin{aligned} &= -(\bar{\rho} a_i \tilde{u}_n)_{,n} + \overline{\rho' u''_{i,n}}\tilde{u}_n - \tilde{u}_n\overline{\rho' u''_{i,n}} - R_{in}\bar{\rho}_{,n} - \bar{\rho}\left(\frac{\overline{\rho u''_i u''_n}}{\bar{\rho}}\right)_{,n} + \overline{\rho u''_n u''_{i,n}} - \bar{\rho} a_n \tilde{u}_{i,n} - \overline{(\rho' u''_n u''_{i,n})} \\ &\quad - b\bar{\sigma}_{ni,n} - \bar{\rho}\overline{\nu' \sigma'_{ni,n}} \end{aligned}$	(136)
Two-Point (LWN)	$\begin{aligned} = &-\left(\overline{\rho'(x+r) u''_i(x-r)}\tilde{u}_n(x+r)\right)_{,n} - R_{in}(x,r)\bar{\rho}_{,n}(x+r) \\ &- \bar{\rho}(x+r)\left(\frac{\overline{\rho(x+r) u''_i(x-r) u''_n(x+r)}}{\bar{\rho}(x+r)}\right)_{,n} + \overline{\rho(x+r) u''_n(x+r) u''_{i,n}(x-r)} \\ &- \overline{\rho'(x+r) u''_n(x-r)}\tilde{u}_{i,n}(x-r) - \overline{\rho'(x+r) u''_n(x-r) u''_{i,n}(x-r)} \\ &+ \overline{\rho'(x+r)\nu'(x-r)}\bar{\sigma}_{ni,n}(x-r) - \frac{\bar{\nu}(x-r)\bar{\rho}(x+r)}{\bar{\nu}(x+r)}\overline{\nu'(x+r)\sigma'_{ni,n}(x-r)} \\ &+ \left\{\overline{\rho'(x+r)\nu'(x-r)\sigma'_{ni,n}(x-r)} - \frac{\bar{\nu}(x-r)}{\bar{\nu}(x+r)}\overline{\nu'(x+r)\rho'(x+r)\sigma'_{ni,n}(x-r)}\right\} \\ &+ \left\{\overline{\rho'(x+r) u''_{i,n}(x-r)}\tilde{u}_n(x+r) - \overline{\rho'(x+r) u''_{i,n}(x-r)}\tilde{u}_n(x-r)\right\} \end{aligned}$	(137)

Note that:

One-Point (BHR)	$\bar{\rho}\left(\frac{\overline{\rho u''_i u''_n}}{\bar{\rho}}\right)_{,n} = \bar{\rho}\left(\frac{\overline{\rho u'_i u'_n}}{\bar{\rho}}\right)_{,n} - \bar{\rho}\left(\frac{\overline{\rho u'_n}}{\bar{\rho}} a_i\right)_{,n} - \bar{\rho}\left(\frac{\overline{\rho u'_i}}{\bar{\rho}} a_n\right)_{,n} = \bar{\rho}\left(\frac{\overline{\rho u'_i u'_n}}{\bar{\rho}}\right)_{,n} - \bar{\rho}\,(a_i a_n)_{,n}$	(138)
Two-Point (LWN)	$\begin{aligned} &\bar{\rho}(x+r)\left(\frac{\overline{\rho(x+r) u''_i(x-r) u''_n(x+r)}}{\bar{\rho}(x+r)}\right)_{,n} \\ &\qquad = \bar{\rho}(x+r)\left(\frac{\overline{\rho(x+r) u'_i(x-r) u'_n(x+r)}}{\bar{\rho}(x+r)}\right)_{,n} \\ &\qquad\quad - \bar{\rho}(x+r)\left(\frac{\bar{\rho}(x-r)}{\bar{\rho}(x+r)}\, a_i(x,r) a_n(x+r,0)\right)_{,n} \end{aligned}$	(139)

One-Point (BHR)	$\left(\frac{\overline{\rho u_i' u_n'}}{\bar{\rho}}\right)_{,n} = \left(\overline{u_i' u_n'}\right)_{,n} + \left(\frac{\overline{\rho' u_i' u_n'}}{\bar{\rho}}\right)_{,n}$	(140)
Two-Point (LWN)	$\left(\frac{\overline{\rho(x+r) u_i'(x-r) u_n'(x+r)}}{\bar{\rho}(x+r)}\right)_{,n} = \left(\overline{u_i'(x-r) u_n'(x+r)}\right)_{,n} + \left(\frac{\overline{\rho'(x+r) u_i'(x-r) u_n'(x+r)}}{\bar{\rho}(x+r)}\right)_{,n}$	(141)

One-Point (BHR)	$= -(\bar{\rho} a_i \tilde{u}_n)_{,n} - R_{in}\bar{\rho}_{,n} - \bar{\rho}\overline{u_i' u_{n,n}'} - \bar{\rho}\left(\frac{\overline{\rho' u_i' u_n'}}{\bar{\rho}}\right)_{,n} + \bar{\rho}\,(a_i a_n)_{,n} - \bar{\rho} a_n \bar{u}_{i,n} - b\bar{\sigma}_{ni,n} - \bar{\rho}\overline{v' \sigma_{n\imath,n}'}$	(142)
Two-Point (LWN)	$\begin{aligned} &= -\left(\overline{\rho'(x+r) u_i''(x-r)}\tilde{u}_n(x+r)\right)_{,n} - R_{in}(x,r)\bar{\rho}_{,n}(x+r) \\ &\quad - \bar{\rho}(x+r)\left(\frac{\overline{\rho'(x+r) u_i'(x-r) u_n'(x+r)}}{\bar{\rho}(x+r)}\right)_{,n} \\ &\quad - \bar{\rho}(x+r)\left(\overline{u_i'(x-r) u_n'(x+r)}\right)_{,n} \\ &\quad + \bar{\rho}(x+r)\left(\frac{\bar{\rho}(x-r)}{\bar{\rho}(x+r)}\, a_i(x,r) a_n(x+r,0)\right)_{,n} + \bar{\rho}(x+r)\overline{u_n'(x+r) u_{i,n}'(x-r)} \\ &\quad + \bar{\rho}(x+r) a_n(x+r,0) a_{i,n}(x-r,0) - \overline{\rho'(x+r) u_n''(x-r)}\bar{u}_{i,n}(x-r) \\ &\quad - \overline{\rho'(x+r) u_n''(x-r)} a_{i,n}(x-r,0) + \overline{\rho'(x+r) v'(x-r)}\bar{\sigma}_{ni,n}(x-r) \\ &\quad - \frac{\bar{v}(x-r)\bar{\rho}(x+r)}{\bar{v}(x+r)}\overline{v'(x+r)\sigma_{n\imath,n}'(x-r)} \\ &\quad + \left\{\overline{\rho'(x+r) v'(x-r)\sigma_{n\imath,n}'(x-r)} - \frac{\bar{v}(x-r)}{\bar{v}(x+r)}\overline{v'(x+r)\rho'(x+r)\sigma_{n\imath,n}'(x-r)}\right\} \\ &\quad + \left\{\overline{\rho'(x+r) u_{i,n}''(x-r)}\tilde{u}_n(x+r) - \overline{\rho'(x+r) u_{i,n}''(x-r)}\tilde{u}_n(x-r)\right\} \\ &\quad + \left\{\overline{\rho'(x+r) u_n''(x+r) u_{i,n}''(x-r)} - \overline{\rho'(x+r) u_n''(x-r) u_{i,n}''(x-r)}\right\} \end{aligned}$	(143)

With some final simplifications we obtain a two-point equation that reduces to the BHR3.1 equations as $r \to 0$, if we assume $u_{n,n}' \approx 0$

One-Point (BHR)	$\begin{aligned} \frac{\partial \bar{\rho} a_i}{\partial t} + (\bar{\rho} a_i \tilde{u}_n)_{,n} &= -R_{in}\bar{\rho}_{,n} - \bar{\rho}\overline{u_i' u_{n,n}'} - \bar{\rho}\left(\frac{\overline{\rho' u_i' u_n'}}{\bar{\rho}}\right)_{,n} + \bar{\rho}\,(a_i a_n)_{,n} - \bar{\rho} a_n \bar{u}_{i,n} - b\bar{\sigma}_{ni,n} \\ &\quad - \bar{\rho}\overline{v' \sigma_{n\imath,n}'} \end{aligned}$	(144)
Two-Point (LWN)	$\begin{aligned} &\frac{\partial \bar{\rho}(x-r) a_i(x,r)}{\partial t} + \left(\bar{\rho}(x-r) a_i(x,r)\tilde{u}_n(x+r)\right)_{,n} \\ &\quad = -R_{in}(x,r)\bar{\rho}_{,n}(x+r) - \bar{\rho}(x+r)\overline{u_{n,n}'(x+r) u_i'(x-r)} \\ &\quad - \bar{\rho}(x+r)\left(\frac{\overline{\rho'(x+r) u_i'(x-r) u_n'(x+r)}}{\bar{\rho}(x+r)}\right)_{,n} \\ &\quad + \bar{\rho}(x+r)\left(\frac{\bar{\rho}(x-r)}{\bar{\rho}(x+r)}\, a_i(x,r) a_n(x+r,0)\right)_{,n} - \bar{\rho}(x-r) a_i(x,r)\bar{u}_{i,n}(x-r) \\ &\quad - b(x,r)\bar{\sigma}_{ni,n}(x-r) - \frac{\bar{v}(x-r)\bar{\rho}(x+r)}{\bar{v}(x+r)}\overline{v'(x+r)\sigma_{n\imath,n}'(x-r)} \\ &\quad + \left\{\overline{\rho'(x+r) v'(x-r)\sigma_{n\imath,n}'(x-r)} - \frac{\bar{v}(x-r)}{\bar{v}(x+r)}\overline{v'(x+r)\rho'(x+r)\sigma_{n\imath,n}'(x-r)}\right\} \\ &\quad + \left\{\overline{\rho'(x+r) u_{i,n}''(x-r)}\left(\tilde{u}_n(x+r) - \tilde{u}_n(x-r)\right)\right\} \\ &\quad + \left\{\overline{\rho'(x+r) u_n''(x+r) u_{i,n}'(x-r)\left(u_n''(x+r) - u_n''(x-r)\right)}\right\} \end{aligned}$	(145)

A.3. b Equation

--- NOTE: This derivation for b isn't fully consistent with the previous two derviations. Use with caution.

This b-equation derivation is in a rougher shape than the other equations and doesn't follow the single point derivation. Additionally, it uses a different definition of a_i. It is included in the hope that it is useful as a reference, but rederiving it following the BHR equations would probably be wise if using the equation for more concrete applications.

To derive the b equations, starting from Clark and Spitz [15] ρ' and v' equations

$$\frac{\partial \rho'}{\partial t} + (\rho'\tilde{u}_n + \rho u''_n)_{,n} = 0$$

$$\frac{\partial v'}{\partial t} + (v'\tilde{u}_n)_{,n} = 2v'(\tilde{u}_n)_{,n} + 2\left(v\, u''_{n,n} - \overline{v\, u''_{n,n}}\right) - (vu''_n - \overline{vu''_n})_{,n}$$

Define $b(x,r) = -\overline{\rho'(x+r)v'(x-r)}$ and $a_j(x,r) = -\overline{\rho(x+r)v'(x-r)u''_n(x+r)}$

$$-\frac{\partial \rho'(x+r)v'(x-r)}{\partial t} = -v'(x-r)\frac{\partial \rho'(x+r)}{\partial t} - \rho'(x+r)\frac{\partial v'(x-r)}{\partial t} = \cdots$$

Two-Point (LWN)	$= \left(v'(x-r)\rho'(x+r)\tilde{u}_n(x+r)\right)_{,n} - \rho'(x+r)\tilde{u}_n(x+r)\, v'_{,n}(x-r)$ $+ \bar{\rho}(x+r)v'(x-r)u''_{n,n}(x+r) + v'(x-r)u''_n(x+r)\bar{\rho}_{,n}(x+r)$ $+ v'(x-r)\rho'_{,n}(x+r)u''_n(x+r) + v'(x-r)\rho'(x+r)u''_{n,n}(x+r)$ $+ \left(\rho'(x+r)v'(x-r)\tilde{u}_n(x-r)\right)_{,n} - v'(x-r)\tilde{u}_n(x-r)\rho'_{,n}(x+r)$ $- 2\rho'(x+r)v'(x-r)\left(\tilde{u}_n(x-r)\right)_{,n} - 2\rho'(x+r)v(x-r)\, u''_{n,n}(x-r)$ $+ 2\rho'(x+r)\overline{v(x-r)\, u''_{n,n}(x-r)} + \bar{v}(x-r)\rho'(x+r)u''_{n,n}(x-r)$ $+ \rho'(x+r)u''_n(x-r)\bar{v}_{,n}(x-r) + \left(v'(x,-r)\rho'(x+r)u''_n(x-r)\right)_{,n}$ $- v'(x-r)\rho'_{,n}(x+r)u''_n(x-r) - \rho'(x+r)\left(\overline{v(x-r)u''_n(x-r)}\right)_{,n}$	(146)

Apply averaging

Two-Point (LWN)	$= -\left(b(x,r)\left(\tilde{u}_n(x+r) + \tilde{u}_n(x-r)\right)\right)_{,n} - \tilde{u}_n(x+r)\overline{\rho'(x+r)v'_{,n}(x-r)}$ $+ \bar{\rho}(x+r)\overline{v'(x-r)u''_{n,n}(x+r)} + \overline{v'(x-r)u''_n(x+r)}\bar{\rho}_{,n}(x+r)$ $+ \overline{v'(x-r)\rho'_{,n}(x+r)u''_n(x+r)} + \overline{v'(x-r)\rho'(x+r)u''_{n,n}(x+r)}$ $+ \bar{\rho}_{,n}(x+r)\overline{\left(v'(x-r)u''_n(x+r)\right)} - \overline{v'(x-r)\tilde{u}_n(x-r)\rho'_{,n}(x+r)}$ $+ 2b(x,r)\left(\tilde{u}_n(x-r)\right)_{,n} - 2\bar{v}(x-r)\overline{\rho'(x+r)\, u''_{n,n}(x-r)}$ $- 2\overline{\rho'(x+r)v'(x-r)u''_{n,n}(x-r)} + \bar{v}(x-r)\overline{\rho'(x+r)u''_{n,n}(x-r)}$ $+ \overline{\rho'(x+r)u''_n(x-r)}\bar{v}_{,n}(x-r) + \left(\overline{v'(x-r)\rho'(x+r)u''_n(x-r)}\right)_{,n}$ $- \overline{v'(x-r)\rho'_{,n}(x+r)u''_n(x-r)}$	(147)

Two-Point (LWN)	$$\begin{aligned} &= -\left(b(x,r)\left(\tilde{u}_n(x+r)+\tilde{u}_n(x-r)\right)\right)_{,n} - \tilde{u}_n(x+r)\overline{\rho'(x+r)v'_{,n}(x-r)} \\ &\quad - \tilde{u}_n(x-r)\overline{v'(x-r)\rho'_{,n}(x+r)} + \bar{\rho}(x+r)\overline{v'(x-r)u''_{n,n}(x+r)} \\ &\quad + \overline{v'(x-r)u''_n(x+r)}\bar{\rho}_{,n}(x+r) + \overline{v'(x-r)\rho'_{,n}(x+r)u''_n(x+r)} \\ &\quad + \overline{v'(x-r)\rho'(x+r)u''_{n,n}(x+r)} + 2b(x,r)\left(\tilde{u}_n(x-r)\right)_{,n} \\ &\quad - 2\bar{v}(x-r)\overline{\rho'(x+r)\,u''_{n,n}(x-r)} - 2\overline{\rho'(x+r)v'(x-r)\,u''_{n,n}(x-r)} \\ &\quad - 2\overline{\rho'(x+r)v'(x-r)u''_{n,n}(x-r)} + \bar{v}(x-r)\overline{\rho'(x+r)u''_{n,n}(x-r)} \\ &\quad + \overline{\rho'(x+r)u''_n(x-r)}\bar{v}_{,n}(x-r) + \left(\overline{v'(x-r)\rho'(x+r)u''_n(x-r)}\right)_{,n} \\ &\quad - \overline{v'(x-r)\rho'_{,n}(x+r)u''_n(x-r)} \end{aligned}$$	(148)

Use

$$-2\bar{v}(x-r)\overline{\rho'(x+r)\,u''_{n,n}(x-r)} + \bar{v}(x-r)\overline{\rho'(x+r)u''_{n,n}(x-r)} = -\bar{v}(x-r)\overline{\rho'(x+r)\,u''_{n,n}(x-r)}$$

Two-Point (LWN)	$$\begin{aligned} &= -\left(b(x,r)\left(\tilde{u}_n(x+r)+\tilde{u}_n(x-r)\right)\right)_{,n} - \tilde{u}_n(x+r)\overline{\rho'(x,r)v'_{,n}(x,-r)} \\ &\quad - \tilde{u}_n(x-r)\overline{v'(x-r)\rho'_{,n}(x+r)} + \bar{\rho}(x+r)\overline{v'(x-r)u''_{n,n}(x+r)} \\ &\quad + \overline{v'(x-r)u''_n(x+r)}\bar{\rho}_{,n}(x+r) + \overline{v'(x-r)\rho'_{,n}(x+r)u''_n(x+r)} \\ &\quad + \overline{v'(x-r)\rho'(x+r)u''_{n,n}(x+r)} + 2b(x,r)\left(\tilde{u}_n(x-r)\right)_{,n} \\ &\quad - \bar{v}(x-r)\overline{\rho'(x+r)\,u''_{n,n}(x-r)} - 2\overline{\rho'(x+r)v'(x-r)u''_{n,n}(x-r)} \\ &\quad + \overline{\rho'(x+r)u''_n(x-r)}\bar{v}_{,n}(x-r) + \left(\overline{v'(x-r)\rho'(x+r)u''_n(x-r)}\right)_{,n} \\ &\quad - \overline{v'(x-r)\rho'_{,n}(x+r)u''_n(x-r)} \end{aligned}$$	(149)

Move advection terms to the LHS

Two-Point (LWN)	$$\begin{aligned} &\frac{\partial b(x,r)}{\partial t} + \left(b(x,r)\left(\tilde{u}_n(x+r)+\tilde{u}_n(x-r)\right)\right)_{,n} - 2b(x,r)\left(\tilde{u}_n(x-r)\right)_{,n} \\ &\quad = -\tilde{u}_n(x+r)\overline{\rho'(x+r)v'_{,n}(x-r)} - \tilde{u}_n(x-r)\overline{v'(x-r)\rho'_{,n}(x+r)} \\ &\quad + \bar{\rho}(x+r)\overline{v'(x-r)u''_{n,n}(x+r)} + \overline{v'(x-r)u''_n(x+r)}\bar{\rho}_{,n}(x+r) \\ &\quad + \overline{v'(x-r)\rho'_{,n}(x+r)u''_n(x+r)} + \overline{v'(x-r)\rho'(x+r)u''_{n,n}(x+r)} \\ &\quad - \bar{v}(x-r)\overline{\rho'(x+r)\,u''_{n,n}(x-r)} - 2\overline{\rho'(x+r)v'(x-r)u''_{n,n}(x-r)} \\ &\quad + \overline{\rho'(x+r)u''_n(x-r)}\bar{v}_{,n}(x-r) + \left(\overline{v'(x-r)\rho'(x+r)u''_n(x-r)}\right)_{,n} \\ &\quad - \overline{v'(x-r)\rho'_{,n}(x+r)u''_n(x-r)} \end{aligned}$$	(150)

Make use of the relations:

$$\rho'(x+r) = \frac{1}{\bar{v}(x+r)}\left(1-\bar{\rho}(x+r)\bar{v}(x+r)-\bar{\rho}(x+r)v'(x+r)-\rho'(x+r)v'(x+r)\right)$$

$$v'(x-r) = \frac{1}{\bar{\rho}(x-r)}\left(1-\bar{\rho}(x-r)\bar{v}(x-r)-\bar{v}(x-r)\rho'(x-r)-\rho'(x-r)v'(x-r)\right)$$

$$b(x,0) = \bar{\rho}(x)\bar{v}(x)-1$$

$$\overline{u''}(x) = -a(x,0)$$

$$\begin{aligned}\bar{v}(x-r)&\overline{\rho'(x+r)\,u''_{n,n}(x-r)}\\&= a_{n,n}(x-r,0)\bar{v}(x-r)\bar{\rho}(x+r)\left[\frac{b(x+r,0)}{b(x+r,0)+1}\right]-\bar{\rho}(x+r)\frac{\bar{v}(x-r)}{\bar{v}(x+r)}\overline{v'(x+r)u''_{n,n}(x-r)}\\&-\frac{\bar{v}(x-r)}{\bar{v}(x+r)}\overline{\rho'(x+r)v'(x+r)u''_{n,n}(x-r)}\end{aligned}$$

$$\begin{aligned}\overline{\big(v'(x-r)\rho'(x+r)u''_n(x-r)\big)}_{,n}&\\&=\bar{\rho}(x+r)\left(\frac{\overline{\big(v'(x-r)\rho'(x+r)u''_n(x-r)\big)}}{\bar{\rho}(x+r)}\right)_{,n}+\frac{\overline{\big(v'(x-r)\rho'(x+r)u''_n(x-r)\big)}}{\bar{\rho}(x+r)}\bar{\rho}_{,n}(x+r)\end{aligned}$$

$$\bar{v}_{,n}(x,-r)=\frac{b_{,n}(x-r,0)}{\bar{\rho}(x-r)}-\frac{b(x-r,0)+1}{\bar{\rho}^2(x-r)}\bar{\rho}_{,n}(x-r)$$

$$\begin{aligned}\bar{\rho}_{,n}(x+r)&\overline{v'(x-r)u''_n(x+r)}\\&=\frac{\bar{\rho}_{,n}(x+r)}{\bar{\rho}(x-r)}\Bigg(-b(x-r,0)\overline{u''_n(x+r)}-\frac{b(x-r,0)+1}{\bar{\rho}(x-r)}\overline{\rho'(x-r)u''_n(x+r)}\\&-\overline{\rho'(x-r)v'(x-r)u''_n(x+r)}\Bigg)\end{aligned}$$

Plug in our relations derived above:

Two-Point (LWN)	$\begin{aligned}&\frac{\partial b(x,r)}{\partial t}+\Big(b(x,r)\big(\tilde{u}_n(x+r)+\tilde{u}_n(x-r)\big)\Big)_{,n}-2b(x,r)\big(\tilde{u}_n(x-r)\big)_{,n}\\&=\left[-\tilde{u}_n(x+r)\overline{\rho'(x+r)v'_{,n}(x-r)}-\tilde{u}_n(x-r)\overline{v'(x-r)\rho'_{,n}(x+r)}\right]\\&+\bar{\rho}(x+r)\overline{v'(x-r)u''_{n,n}(x+r)}+\bar{\rho}(x+r)\frac{\bar{v}(x-r)}{\bar{v}(x+r)}\overline{v'(x+r)u''_{n,n}(x-r)}\\&+\frac{\bar{\rho}_{,n}(x+r)}{\bar{\rho}(x-r)}\left(-b(x-r,0)\overline{u''_n(x+r)}-\frac{b(x-r,0)+1}{\bar{\rho}(x-r)}\overline{\rho'(x-r)u''_n(x+r)}\right)\\&+\overline{v'(x-r)\rho'_{,n}(x+r)u''_n(x+r)}-\overline{v'(x-r)\rho'_{,n}(x+r)u''_n(x-r)}\\&+\overline{v'(x-r)\rho'(x+r)u''_{n,n}(x+r)}+\frac{\bar{v}(x-r)}{\bar{v}(x+r)}\overline{\rho'(x+r)v'(x+r)u''_{n,n}(x-r)}\\&-2\overline{\rho'(x,r)v'(x,-r)u''_{n,n}(x,-r)}\\&-a_{n,n}(x-r,0)\bar{v}(x-r)\bar{\rho}(x+r)\left[\frac{b(x+r,0)}{b(x+r,0)+1}\right]\\&+\overline{\rho'(x+r)u''_n(x-r)}\left[\frac{b_{,n}(x-r,0)}{\bar{\rho}(x-r)}-\frac{b(x-r,0)+1}{\bar{\rho}^2(x-r)}\bar{\rho}_{,n}(x-r)\right]\\&+\bar{\rho}(x+r)\left(\frac{\overline{\big(v'(x-r)\rho'(x+r)u''_n(x-r)\big)}}{\bar{\rho}(x+r)}\right)_{,n}+\\&\bar{\rho}_{,n}(x+r)\left[\frac{\overline{\big(\rho'(x+r)v'(x-r)u''_n(x-r)\big)}}{\bar{\rho}(x+r)}-\frac{\overline{\rho'(x-r)v'(x-r)u''_n(x+r)}}{\bar{\rho}(x-r)}\right]\end{aligned}$	(151)

Change to advection of ρb

Two-Point (LWN)	$\begin{aligned} &\frac{\partial \bar{\rho}(x) b(x,r)}{\partial t} + \left(\bar{\rho}(x) b(x,r) \frac{\left(\tilde{u}_n(x+r)+\tilde{u}_n(x-r)\right)}{2}\right)_{,n} = \\ &-\bar{\rho}(x) b(x,r)\left[\tilde{u}_{n,n}(x) - 2\tilde{u}_{n,n}(x-r) + \frac{\left(\tilde{u}_{n,n}(x+r)+\tilde{u}_{n,n}(x-r)\right)}{2}\right] \\ &+ b(x,r)\left(\frac{\tilde{u}_n(x+r)+\tilde{u}_n(x-r)}{2} - \tilde{u}_n(x)\right)\bar{\rho}_{,n}(x) \\ &-\bar{\rho}(x)\Bigg[\frac{\left(\tilde{u}_n(x+r)+\tilde{u}_n(x-r)\right)}{2} b_{,n}(x,r) + \tilde{u}_n(x+r)\overline{\rho'(x+r)v'_{,n}(x-r)} \\ &\quad + \tilde{u}_n(x-r)\overline{v'(x-r)\rho'_{,n}(x+r)}\Bigg] \\ &+\bar{\rho}(x)\left[\bar{\rho}(x+r)\overline{v'(x-r)u''_{n,n}(x+r)} + \bar{\rho}(x+r)\frac{\bar{v}(x-r)}{\bar{v}(x+r)}\overline{v'(x+r)u''_{n,n}(x-r)}\right] \\ &+\bar{\rho}(x)\left[\overline{v'(x-r)\rho'_{,n}(x+r)u''_n(x+r)} - \overline{v'(x-r)\rho'_{,n}(x+r)u''_n(x-r)}\right] \\ &+\bar{\rho}(x)\Bigg[\overline{v'(x-r)\rho'(x+r)u''_{n,n}(x+r)} + \frac{\bar{v}(x-r)}{\bar{v}(x+r)}\overline{\rho'(x+r)v'(x+r)u''_{n,n}(x-r)} \\ &\quad - 2\overline{\rho'(x+r)v'(x-r)u''_{n,n}(x-r)}\Bigg] \\ &-\bar{\rho}(x) a_{n,n}(x-r,0)\left[\bar{v}(x-r)\bar{\rho}(x+r)\left[\frac{b(x+r,0)}{b(x+r,0)+1}\right] - b(x,r)\right] \\ &+\bar{\rho}(x)\left[\frac{\overline{\rho'(x+r)u''_n(x-r)}}{\bar{\rho}(x-r)} b_{,n}(x-r,0) + a_n(x-r,0) b_{,n}(x,r)\right] \\ &-\bar{\rho}(x)\overline{\rho'(x+r)u''_n(x-r)}\left[\frac{b(x-r,0)+1}{\bar{\rho}^2(x-r)}\right]\bar{\rho}_{,n}(x-r) \\ &-\bar{\rho}(x)\Bigg[\frac{b(x,r)}{\bar{\rho}(x+r)} a_n(x-r,0) - \frac{b(x-r,0)}{\bar{\rho}(x-r)} a_n(x+r,0) \\ &\quad + \frac{b(x-r,0)+1}{\bar{\rho}^2(x-r)}\overline{\rho'(x-r)u''_n(x+r)}\Bigg]\bar{\rho}_{,n}(x+r) \\ &+\bar{\rho}(x)\bar{\rho}(x+r)\left(\frac{\overline{\left(v'(x-r)\rho'(x+r)u'_n(x-r)\right)}}{\bar{\rho}(x+r)}\right)_{,n} + \\ &\bar{\rho}(x)\bar{\rho}_{,n}(x+r)\left[\frac{\overline{\left(\rho'(x+r)v'(x-r)u''_n(x-r)\right)}}{\bar{\rho}(x+r)} - \frac{\overline{\rho'(x-r)v'(x-r)u''_n(x+r)}}{\bar{\rho}(x-r)}\right] \end{aligned}$	(152)

Rearranging to have zero production terms at the end yields a form that asymptotes to the BHR3.1 form as $r \to 0$. Again, note the caveats that this equation uses a different form of a_i than used elsewhere in the report.

Single-Point (BHR)	$\frac{\partial(\bar{\rho}b)}{\partial t} + (\bar{\rho}b\tilde{u}_n)_{,n} = -2(b+1)a_n\bar{\rho}_{,n} + 2\bar{\rho}a_n b_{,n} + \bar{\rho}\left(\frac{\overline{(\rho' v' u'_n)}}{\bar{\rho}}\right)_{,n} + 2\bar{\rho}\overline{v' u''_{n,n}}$	(153)
Two-Point (LWN)	$\begin{aligned} &\frac{\partial \bar{\rho}(x)b(x,r)}{\partial t} + \left(\bar{\rho}(x)b(x,r)\frac{(\tilde{u}_n(x+r)+\tilde{u}_n(x-r))}{2}\right)_{,n} \\ &= \bar{\rho}(x)\Big[\bar{\rho}(x+r)\overline{v'(x-r)u''_{n,n}(x+r)} \\ &+ \bar{\rho}(x+r)\frac{\bar{v}(x-r)}{\bar{v}(x+r)}\overline{v'(x+r)u''_{n,n}(x-r)}\Big] \\ &+ \bar{\rho}(x)\left[\frac{\overline{\rho'(x+r)u''_n(x-r)}}{\bar{\rho}(x-r)}b_{,n}(x-r,0) + a_n(x-r,0)b_{,n}(x,r)\right] \\ &- \bar{\rho}(x)\left(\frac{b(x-r,0)+1}{\bar{\rho}^2(x-r)}\right)\Big(\overline{\rho'(x+r)u''_n(x-r)}\bar{\rho}_{,n}(x-r) \\ &+ \overline{\rho'(x-r)u''_n(x+r)}\bar{\rho}_{,n}(x+r)\Big) \\ &+ \bar{\rho}(x)\bar{\rho}(x+r)\left(\frac{\overline{(v'(x-r)\rho'(x+r)u'_n(x-r))}}{\bar{\rho}(x+r)}\right)_{,n} \\ &- \bar{\rho}(x)b(x,r)\left[\tilde{u}_{n,n}(x) - 2\tilde{u}_{n,n}(x-r) + \frac{(\tilde{u}_{n,n}(x+r)+\tilde{u}_{n,n}(x-r))}{2}\right] \\ &+ b(x,r)\left(\frac{\tilde{u}_n(x+r)+\tilde{u}_n(x-r)}{2} - \tilde{u}_n(x)\right)\bar{\rho}_{,n}(x) \\ &- \bar{\rho}(x)\Big[\frac{(\tilde{u}_n(x+r)+\tilde{u}_n(x-r))}{2}b_{,n}(x,r) + \tilde{u}_n(x+r)\overline{\rho'(x+r)v'_{,n}(x-r)} \\ &+ \tilde{u}_n(x-r)\overline{v'(x-r)\rho'_{,n}(x+r)}\Big] \\ &+ \bar{\rho}(x)\left[\overline{v'(x-r)\rho'_{,n}(x+r)(u''_n(x+r)-u''_n(x-r))}\right] \\ &+ \bar{\rho}(x)\Big[\overline{v'(x-r)\rho'(x+r)u'_{n,n}(x+r)} \\ &+ \frac{\bar{v}(x-r)}{\bar{v}(x+r)}\overline{\rho'(x+r)v'(x+r)u'_{n,n}(x-r)} - 2\overline{\rho'(x+r)v'(x-r)u'_{n,n}(x-r)}\Big] \\ &- \bar{\rho}(x)\, b(x,r)\left(a_{n,n}(x-r,0) - a_{n,n}(x+r,0)\right) \\ &+ \bar{\rho}(x)\bar{\rho}_{n}(x+r)\Big[\frac{\overline{(\rho'(x+r)v'(x-r)u'_n(x-r))}}{\bar{\rho}(x+r)} \\ &- \frac{\overline{\rho'(x-r)v'(x-r)u'_n(x+r)}}{\bar{\rho}(x-r)}\Big] \end{aligned}$	(154)